MTL MS 86-3

AD

AD-A184 791

WORK-IN-PROGRESS PRESENTED AT THE ARMY SYMPOSIUM ON SOLID MECHANICS, 1986 - LIGHTENING OF THE FORCE

DTIC
ELECTE
SEP 2 2 1987
D
D

October 1986

US ARMY
LABORATORY COMMAND
MATERIALS TECHNOLOGY
LABORATORY

U.S. ARMY MATERIALS TECHNOLOGY LABORATORY
Watertown, Massachusetts 02172-0001

87 9 15 07

The findings in this report are not to be construed as an official Department of the Army position, unless so designated by other authorized documents.

Mention of any trade names or manufacturers in this report shall not be construed as advertising nor as an official indorsement or approval of such products or companies by the United States Government.

REPORT DOCUMENTATION PAGE		READ INSTRUCTIONS BEFORE COMPLETING FORM
1. REPORT NUMBER MTL MS 86-3	2. GOVT ACCESSION NO. *ADA184791*	3. RECIPIENT'S CATALOG NUMBER
4. TITLE *(and Subtitle)* WORK-IN-PROGRESS PRESENTED AT THE ARMY SYMPOSIUM ON SOLID MECHANICS, 1986 - LIGHTENING OF THE FORCE		5. TYPE OF REPORT & PERIOD COVERED Final Report
		6. PERFORMING ORG. REPORT NUMBER
7. AUTHOR(s)		8. CONTRACT OR GRANT NUMBER(s)
9. PERFORMING ORGANIZATION NAME AND ADDRESS U.S. Army Materials Technology Laboratory Watertown, Massachusetts 02172-0001 SLCMT-MSR		10. PROGRAM ELEMENT, PROJECT, TASK AREA & WORK UNIT NUMBERS
11. CONTROLLING OFFICE NAME AND ADDRESS U.S. Army Laboratory Command 2800 Powder Mill Road Adelphi, Maryland 20783-1145		12. REPORT DATE October 1986
		13. NUMBER OF PAGES 67
14. MONITORING AGENCY NAME & ADDRESS(*if different from Controlling Office*)		15. SECURITY CLASS. *(of this report)* Unclassified
		15a. DECLASSIFICATION/DOWNGRADING SCHEDULE

16. DISTRIBUTION STATEMENT *(of this Report)*

Approved for public release; distribution unlimited.

17. DISTRIBUTION STATEMENT *(of the abstract entered in Block 20, if different from Report)*

18. SUPPLEMENTARY NOTES

19. KEY WORDS *(Continue on reverse side if necessary and identify by block number)*

SEE REVERSE

20. ABSTRACT *(Continue on reverse side if necessary and identify by block number)*

Work-In-Progress presented at the Army Symposium on Solid Mechanics, 1986 - Lightening of the Force, held at the U.S. Military Academy, West Point, New York, 7-9 October 1986.

DD ₁ ᶠᴼᴿᴹ₇₃ 1473   EDITION OF 1 NOV 65 IS OBSOLETE

Block No. 19

KEY WORDS

Acceleration	Gunfire	Rotating Bands
Adhesives	Guns	Rotor Blades
Aircraft	Helicopters	Shaped Charges
Airframes	High Temperature	Shear Properties
Aluminum Alloys	Impact	Shelters
Ballistics	Inertia	Ships
Ceramic Materials	Intensity	Shock (Mechanics)
Collisions	Joining	Spectra
Composite Materials	Joints	Statistical Anslysis
Computerized Simulation	Kinetic Energy	Strain (Mechanics)
Confidence Level	Landing Gear	Strain Rate
Copper	Life (Durability)	Strength (General)
Corrosion	Lightweight	Stress Corrosion
Crack Propagation	Loads (Forces)	Stresses
Crashes	Measurement	Structural Response
Crash Resistance	Mechanics	Structures
Defects (Materials)	Metals	Survival (General)
Displacements	Mines (Ordnance)	Telemeter Systems
Dynamic Response	Models	Temperatures
Dynamics	Moisture	Thermal Stresses
Energy Absorbers	Nondestructive Testing	Threats
Environments	Plastic Properties	Time Dependence
Explosives	Plates	Titanium
Fabrication	Predictions	Transients
Failure	Pressure	Vibration
Fatigue (Materials)	Probability	Vulnerability
Fighter Aircraft	Projectiles	Weapon Systems
Fragmentation	Protection	
Fuselages	Reliability	

QUALITY INSPECTED 2

Accesion For

NTIS CRA&I	✓	
DTIC TAB	☐	
Unannounced	☐	
Justification		

By

Distribution /

Availability Codes

Dist	Avail and / or Special
A-1	

PREFACE

The Army Symposium on Solid Mechanics, 1986, represents the tenth in the series of bienniel meetings of researchers from government, academia and industry working in the field of solid mechanics in support of Army, Navy and Air Force systems.

This document contains the extended abstracts of work-in-progress selected for presentation at the 1986 symposium and inclusion in the proceedings. A companion document contains the full technical manuscripts of completed work selected for presentation at the meeting.

Initially organized in 1966 to answer the needs of Army researchers for a forum for presentation and critical review of work being accomplished by Army laboratories and their contractors, the symposium was expanded in 1968 to include the participation of the Navy, Air Force and other government agencies active in areas of Army interest. During the ensuing years the symposium fulfilled its original purpose by providing an excellent opportunity for the interaction of mechanics researchers in the three services as well as the Departments of Energy and Transportation.

For each meeting the symposium committee selects a central theme representing a technical or system-related area of current major interest to the Army. The theme "Lightening of the Force" selected for this, the tenth symposium, represents a major Army priority in order to enhance both fighting capability on the battlefield and the capability for rapid deployment of fighting forces to remote locations. The full papers and extended abstracts selected for presentation and/or inclusion in the proceedings are representative of the extensive research and advance development being carried on in support of this central theme.

Although centered on the applied research (6.2) area, the area of interest of the symposium spans the range from basic (6.1) research through advanced development (6.4). The papers selected for this symposium provide this broad mixed coverage of the central theme.

On this tenth anniversary a review of the record of the Army Symposium on Solid Mechanics shows that it is an appropriate and popular event that has filled an important need over the twenty years of its existence. It is fitting now to acknowledge the foresight and guidance of the individuals who initiated and steadfastly supported the symposium from the beginning. Therefore to Joseph I. Bluhm, who throughout his career was the leading advocate of solid mechanics research and engineering in the Army; and to the late Dr. John M. Slepetz who led and guided the Army Materials Technology Laboratory and the Army to and through the intricacies of advanced composites.

Proceedings of the Army Symposium on Solid Mechanics, 1968,   AMMRC
MS 68-09, September 1968, AD 675 463

Proceedings of the Army Symposium on Solid Mechanics, 1970:
Lightwieght Structures,
AMMRC MS 70-5, December 1970, AD 883 455L

Proceedings of the Army Symposium on Solid Mechanics, 1972:
The Role of Mechanics in Design - Ballistic Problems,
AMMRC MS 73-2, September 1973, AD 772 827

Work-In-Progress Presented at the Army Symposium on Solid Mechanics, 1974:
The Role of Mechanics in Design, Structural Joints,
AMMRC MS 74-9, September 1974, AD 786 524

Work-In-Progress Presented at the Army Symposium on Solid Mechanics, 1976:
Composite Materials: The Influence of Mechanics of Failure on Design,
AMMRC MS 76-3, September 1976, AD A029 736

Ongoing Case Studies Presented at the Army Symposium on Solid Mechanics, 1978:
Case Studies on Structural Integrity and Reliability
AMMRC MS 78-4, September 1978, AD A059 605/6G1

Work-In-Progress Presented at the Army Symposium on Solid Mechanics, 1980:
Designing for Extremes: Environment, Loading, and Structural Behavior,
AMMRC MS 80-5, September 1980, AD A090685

Work-In-Progress Presented at the Army Symposium on Solid Mechanics, 1982:
Critical Mechanics Problems in Systems Designs,
AMMRC MS 82-5, September 1982 AD A119497

Proceedings of the Army Symposium on Solid Mechanics, 1984:
Advances in Solid Mechanics,
AMMRC MS 84-3, September 1984 AD A150042

CONTENTS

COMPUTED NEUTRON TOMOGRAPHY
AND
CODED APERTURE HOLOGRAPHY
FROM REAL TIME NEUTRON IMAGES

*

MARK F. SULCOSKI
University of Virginia
P. O. Box 7432
Charlottesville, Virginia 22906

EXTENDED ABSTRACT

Neutron radiography is well known as a non-destructive examination (NDE) technique for low atomic number materials. The increased interest in lightweight composite materials using low atomic number elements (such as carbon) require modern imaging techniques such as computed neutron tomography and coded aperture neutron holography to complement other NDE techniques. The unique interaction mechanisms of neutron radiation as compared to x-rays allow higher detection structures, adhesive bonding layers in laminated structures and delamination detection in composite structures.

The purpose of the continuing work described herein is to develop and investigate the uses of neutron tomography and holography for NDE applications. Much of the early work in neutron tomography was limited by slow and tedious methods of optical densitometer scanning of static neutron radiographs to obtain data. The use of boron trifluoride counters rather than film improved the usefulness. This paper describes the use of a real time neutron imaging system coupled with a dedicated image processing system to obtain neutron tomographs.

Experiments to date have utilized a Thomson-CSF neutron camera coupled to a Digital Equipment Corporation LSI 11/23 based system used for image processing. Experiments have included the following:

    Configuration of a reactor neutron beam port for neutron
    imaging.

    Development and implementation of a convolution method
    tomographic algorithm suitable for neutron imaging.

Results to date have demonstrated the proof of principal of this neutron tomography system:

Tomographs from real time images of 1.6 cm (0.63 in) wooden
test objects have achieved near theoretical resolution of
1.3 mm (0.051 in) voids using 200 projections with no image
processing.

Computation time of approximately 30 seconds per projection.

Preliminary benefits of image processing before tomography
data acquisition investigated.

Future work is planned to include the following:

Investigation of alternate algorithms to reduce the number
of projections necessary for a given resolution.

Investigation of combinations of image processing techniques
and other data preprocessing algorithms to allow larger
objects to be imaged and to increase resolution.

More studies of void detection and delamination detection
for various materials and structures.

Coded aperture neutron holography is under investigation using a
cadmium Fresnel zone plate as the coded aperture and the real time
imaging system as the detection and holographic reconstruction system.
Coded aperture imaging utilizes the zone place to encode scattered
neutron radiation from the entire volume of an object. The scattered
radiation pattern recorded at the detector is used as input data to a
convolution algorithm which reconstructs the scattering source (object).
Thus, ideally, all the tomography planes of the object are recorded
simultaneously allowing a three dimensional neutron image of the object.
This technique has not yet been successfully implemented and is
still under development. Current ongoing work includes:

Investigation of techniques to increase object scattered
neutron flux and/or increased detector sensitivity.

Comparison of several methods to improve signal-to-noise
ratio of the neutron detection system.

*

Present address: U. S. Army Foreign Science and
                         Technology Center
                    220 Seventh Street N. E.
                    Charlottesville, Virginia 22901

SPATIAL STRENGTH VARIATION AND STATISTICAL SIZE EFFECT OF LAMINATED ORTHOTROPIC COMPOSITE MATERIALS

ELIAS SAMARAS
Assistant Professor of Civil Engineering

MASANOBU SHINOZUKA
Renwick Professor of Civil Engineering

Both at the Department of Civil Engineering and Engineering Mechanics
Columbia University, New York, NY 10027

ABSTRACT

Resisting strength and other properties of engineering materials used for the production of laminated orthotropic composites arc known to have considerable spatial variations. In the present study, a particular emphasis is placed, however, on the probabilistic model for spatial variation of material strength and on the corresponding statistical size effect. The principal idea lies in the interpretation that the material strength can be idealized as a multidimensional random field. This interpretation together with the recently developed method of digital simulation of multidimensional random fields by use of ARMA models makes it possible to demonstrate the statistical size effect in terms of numerical examples. Tha ARMA model method mentioned above uses a recursive equation whose coefficient matrices are determined in accordance with the prescribed autocorrelation function of the multidimensional random field. Using the recursive equation with these coefficient matrices, we can generate with substantial computational ease, sample functions of the field over a large two- or three- dimensional domain. An alternative method for the digital simulation of multidimensional random fields is the well-known Fast Fourier Transform (FFT) method. It should be pointed out however, that the ARMA model method is consider-

ably more efficient in terms of computational time.

Consider now a specific example of a laminated orthotropic composite plate consisting of two laminae. Each lamina is divided into an equal number of elements ($4 \cdot 6 = 24$ for the case considered – see Fig. 1).
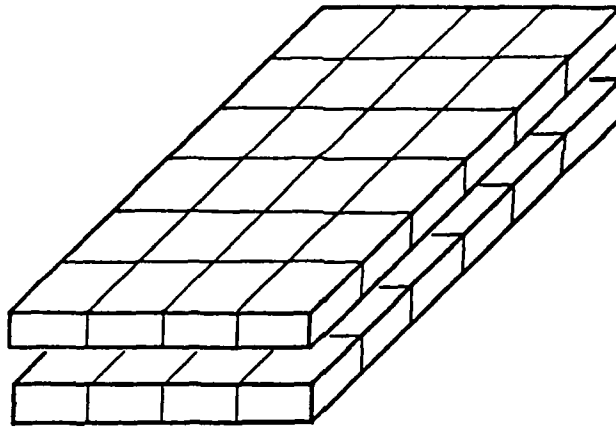
Fig. 1   Division of plate into 48 elements

Therefore the whole plate is divided into $2 \cdot 24 = 48$ elements. We can now assign values for the material strengths in the three principal directions (longitudinal, transverse and shear strengths respectively) for each one of the 48 elements. This can be achieved by considering that for each lamina the material strengths in the three principal directions consist a three-variate two-dimensional (3V-2D) random field. In this way, each one of the 48 elements is assigned with a different triad of values for the material strengths in the three principal directions.

Considering now uniaxial stress of the laminated orthotropic composite plate, we can start from a very small stress-level σ and check whether one or more of the 48 elements fail under the given stress σ. The Tsai-Hill failure criterion shown below in Eq. (a), can be used to perform this check. It should be noted that this failure check is performed 48 times, once for each element. The Tsai-Hill failure criterion is given by :

4

$$\frac{cos^4\theta}{X^2} + (\frac{1}{S^2} - \frac{1}{X^2})cos^2\theta sin^2\theta + \frac{sin^4\theta}{Y^2} = \frac{1}{\sigma^2} \qquad (a)$$

where X, Y, S are the strengths in the three principal directions (longitudinal, transverse and shear respectively), σ is the externally applied axial stress and θ is the angle between the principal direction X and the direction of application of the uniaxial stress σ. Of course, any other failure criterion can be used instead of the Tsai-Hill one, by making slight modifications to the above procedure. For example some other failure criterion might involve only two independent strengths instead of the three of the Tsai-Hill criterion. In this case, a two-variate two-dimensional random field has to be generated.

If no failure is detected at the original stress-level, the stress-level can be increased by steps up to the point where some element(s) fails for the first time. The value of the externally applied uniaxial stress at this level can be considered as the strength of the whole laminated orthotropic composite plate in uniaxial tension.

Using Monte Carlo techniques the above-described procedure can be repeated a number of times for different realizations of the 3V-2D random field describing the strengths of the laminated composite plate in the three pricipal directions. In this fashion several different values for the strength of the whole laminated plate can be obtained. Then, the distribution function of those values can be estimated by the use of some test of goodness of fit (e.g. probability paper).

Finally, in order to examine the statistical size effect, the following procedure can be followed. The same problem as the one described above to find the strength of the whole laminated composite plate is solved again by considering in the beginning twice the area of the original laminated plate, then thrice and so on, however always using the same autocorrelation function for the 3V-2D random field describing the material strength variability in the three principal directions. In this way, conclusions can be drawn about the statistical size effect due to the spatial strength variation.

5

A DIRECT METHOD TO OBTAIN CONSTITUTIVE MODEL CONSTANTS FROM CYLINDER IMPACT TEST RESULTS

TIM J. HOLMQUIST
Development Engineer

GORDON R. JOHNSON
Principal Engineering Fellow
Honeywell Defense Systems Division
Edina, MN 55436

INTRODUCTION

The cylinder impact test was introduced by G. I. Taylor in 1948. Since that time the merits of this test have been debated. Some would argue that this test should not be used to obtain constitutive data because a wide range of unknown strains, strain rates, temperatures, and stresses vary throughout the test specimen, and throughout the duration of the test. It is better, they would say, to obtain data from dynamic tension, compression, and/or torsion tests, in which the variables are better defined, and then use the cylinder impact test to provide an independent check of the data.

Others would argue that dynamic tension, compression, and/or torsion tests require expensive test facilities and that these tests are limited in their ability to achieve the range of strains and strain rates of interest. Conversely, the cylinder impact test is simple, inexpensive, and provides data for the appropriate range of strains and strain rates. During the past twenty years, several researchers have used this test to estimate dynamic flow stresses for various materials.

The work reported in this paper is directed at developing an *explicit method* (as opposed to previous trial-and-error methods) to obtain constants for computational constitutive models.

DISCUSSION AND RESULTS

Figure 1 shows a comparison of cylinder impact test results and corresponding EPIC-2 computational results for OFHC copper. The test data are from Reference 1 (Johnson and Cook, *Proceedings of the Seventh International Symposium on Ballistics*, 1983). The adiabatic stress-strain relationships are given in Figure 2 and the strength model constants used for the four cases are given in Table I. The adiabatic stresses are shown only to the maximum strains attained in the computed results.
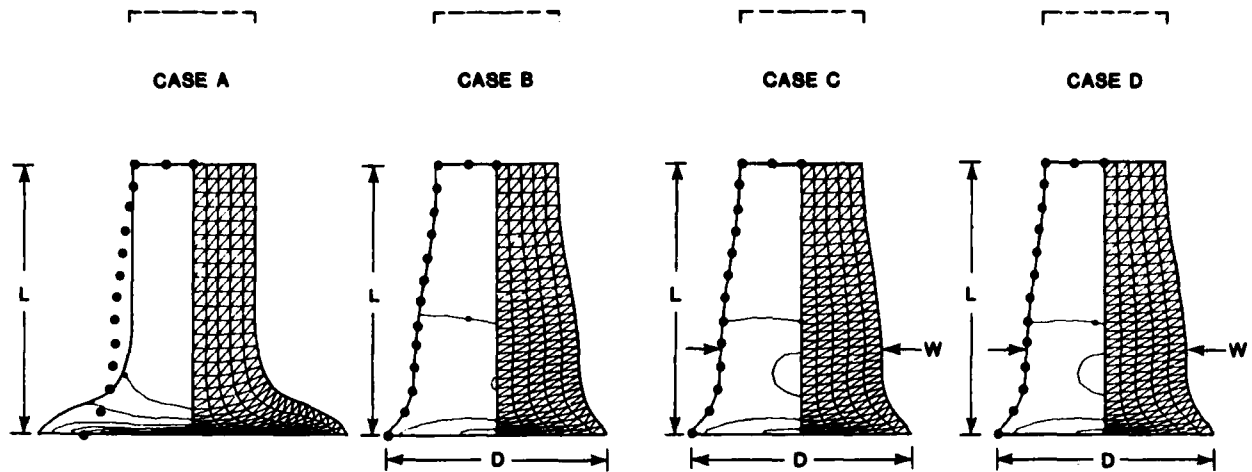
NOTES:

- OFHC COPPER CYLINDER ($L_o = 25.4mm$, $D_o = 7.6mm$, $L = 16.2mm$, $D = 13.5mm$)
- IMPACT VELOCITY = 190 m/s
- TEST RESULTS INDICATED BY DOTS ••••
- EQUIVALENT PLASTIC STRAIN CONTOURS SHOWN AT INTERVALS OF 0.5

Figure 1. Comparison of Test Results with Computed Results Using Various Strength Model Constants
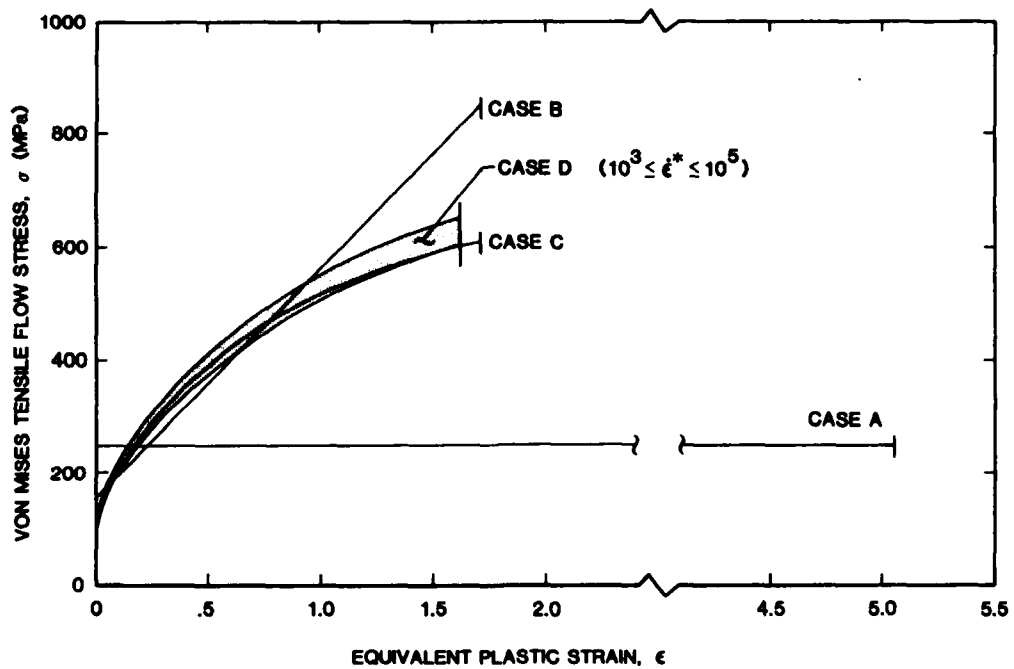

Figure 2. Adiabatic Stress-Strain Relationships for the Various Strength Models

8

Table I. Strength Model Constants for the Computed Results

		CASE A	CASE B	CASE C	CASE D
STRENGTH CONSTANTS FOR $\sigma = [A + B\epsilon^n][1 + C \ln \dot{\epsilon}^*][1 - T^{*m}]$					
A	(MPa)	250	160	103	98
B	(MPa)	0.	400	469	368
n		–	1.00	.65	.70
C		0.	0.	0.	.025
m		–	–	1.00	1.09
$\dot{\epsilon}^* = \dot{\epsilon}/\dot{\epsilon}_0$ FOR $\dot{\epsilon}_0 = 1.0 \text{ S}^{-1}$ $T^* = (T - T_{ROOM}) / (T_{MELT} - T_{ROOM})$					

For Case A the length, L, of the deformed cylinder is matched with the computational result. Because only one deformed dimension is matched, only one independent strength constant (representing a constant flow stress) can be obtained. It can be seen that there are significant discrepancies between the test and computational results at the deformed end of the cylinder.

Case B provides for linear strain hardening. By matching both the deformed length, L, and the maximum diameter, D, it is possible to obtain the two constants for the linear hardening. Here the computed result is in good general agreement with the test result. If this model would be applied to larger strains than those experienced in the computed results of Case B, however, it would probably lead to excessively high stresses. It is well known that thermal softening tends to decrease the rate of strain hardening at large strains. In general, if the basic model accurately represents material behavior, then the results can probably be extrapolated beyond the data base.

Cases C and D are based on the following model for the von Mises tensile flow stress (Reference 1):

$$\sigma = [A + B\epsilon^n][1 + C\ln \dot{\epsilon}^*][1 - T^{*m}] \tag{1}$$

where ϵ is the equivalent plastic strain, $\dot{\epsilon}^* = \dot{\epsilon}/\dot{\epsilon}_0$ is the dimensionless plastic strain rate for $\dot{\epsilon}_0 = 1.0\text{s}^{-1}$, and T^* is the homologous temperature. The five material constants are A, B, n, C, m. The first three constants (A, B, n) represent the strain hardening characteristics of the material and are the ones which are determined from the test results. Because there are now three constants, it is possible to match three deformed dimensions—the length, L, the maximum diameter, D, and an intermediate diameter, W. The strain rate constant, C, and the thermal softening constant, m, must be approximated or obtained from other sources.

Case C is the result obtained if nothing is known about the strain rate or thermal softening characteristics of the material. Here, the strain rate constant is set to $C = 0$, and the thermal softening is assumed to be linear, or $m = 1.0$. Case D uses strain rate and thermal softening data from Reference 1. Even though there is little apparent difference between Cases C and D for this problem, for some other problems (with wider ranges of strain rates and temperatures) the Case D constants will probably provide better results.

METHOD TO OBTAIN CONSTANTS

The method consists of applying the following equation in an iterative manner until a satisfactory set of constants is attained:

$$\{\Delta x\} = [K]\{\Delta y\} \tag{2}$$

$$\text{where } \{\Delta x\} = \begin{Bmatrix} \Delta A \\ \Delta B \\ \Delta n \end{Bmatrix} \text{ and } \{\Delta y\} = \begin{Bmatrix} \Delta L \\ \Delta D \\ \Delta W \end{Bmatrix}.$$

For a given set of material constants (A, B, n) it is possible to compute the deformed geometrical dimensions (L, D, W). These deformed dimensions are compared to the dimensions of the test specimen and the differences are expressed as ΔL, ΔD, and ΔW. These differences can then be used to find the corresponding material constant changes which will lead to improved material constants. This is accomplished through a 3 x 3 operator matrix, [K], where K_{ij} is the change in material constant, Δx_i, due to a unit change in the deformed geometry, Δy_j.

The operator matrix, [K], can most easily be attained by first developing the inverse to this matrix. This is accomplished by running a series of four computer simulations with different material model constants. The first simulation is a baseline computation which uses an initial estimate of the constants. The next three simulations vary each of the three constants independently (A', B', n'). This procedure, and the generation of the $[K]^{-1}$, is shown in Figure 3.

The operator matrix assumes a linear relationship between incremental material constant changes and incremental deformed dimension changes. This is not a valid assessment because the operator matrix is actually nonlinear. However, the linear assumption can produce accurate, converging results if the four simulations used to generate the operator matrix are sufficiently close to the final solution.

For the limited number of solutions obtained to date, convergence was experienced after several iterations. In these cases, the initial operator matrix was used for all iterations. The rate of convergence can eventually be increased by implementing improved techniques that continually update the operator matrix after every simulation.

SIMULATION	MATERIAL CONSTANTS				DEFORMED CYLINDER DIMENSIONS		
1 (BASELINE)	A	B	n	$\longrightarrow$	L_1	D_1	W_1
2	A'	B	n	$\longrightarrow$	L_2	D_2	W_2
3	A	B'	n	$\longrightarrow$	L_3	D_3	W_3
4	A	B	n'	$\longrightarrow$	L_4	D_4	W_4

$$
[\kappa]^{-1} = \begin{bmatrix}
\dfrac{L_1 - L_2}{A - A'} & \dfrac{L_1 - L_3}{B - B'} & \dfrac{L_1 - L_4}{n - n'} \\[2ex]
\dfrac{D_1 - D_2}{A - A'} & \dfrac{D_1 - D_3}{B - B'} & \dfrac{D_1 - D_4}{n - n'} \\[2ex]
\dfrac{W_1 - W_2}{A - A'} & \dfrac{W_1 - W_3}{B - B'} & \dfrac{W_1 - W_4}{n - n'}
\end{bmatrix}
$$

Figure 3. Summary of Computer Simulations Required to Generate Inverse of Operator Matrix

SUMMARY AND CONCLUSIONS

It has been demonstrated that it is possible to directly obtain constitutive model constants from cylinder impact test results. Future work will be directed at improving the convergence of the method, and applying the method to other models and materials.

ACKNOWLEDGEMENT

11

PLASTIC STRAIN LOCALIZATION BETWEEN VOIDS
IN SHEAR DEFORMATION FIELDS

D. M. Tracey, C. E. Freese, and P. J. Perrone

U. S. Army Materials Technology Laboratory
Watertown, Massachusetts, 02172-0001

ABSTRACT

Metallographic studies[1] have shown that crack propagation occurs by a plastic shear instability mechanism in high strength martensitic alloy steels. On the microscale, propagation occurs in a non-planar fashion following bands which develop along the shear directions. Voids evidently play a major role in this fracture process, with microcracks developing between interacting voids. In shear tests of high strength 4340 steel[2], voids have been found within shear bands at debonded sub-micron sized grain refinement particles. It has been speculated that the microcracks linking such voids form as a result of the coalescence of voids which nucleate at smaller scale strengthening particles. It is likely that this secondary void nucleation results from the strain intensification caused by the dominant voids. Fracture is expected after a critical number of microcracks are formed.

The present mechanics study is being conducted in suppor an alloy development research program attempting to produce ultra-high strength steel alloy (300-350 ksi) with fracture toughness sufficiently high (60-120 ksi$\sqrt{in}$) to allow a wide range of structural applications. Success of this program will provide an important new material selection option for lightweight fracture resistant metallic structures. The mechanics work is directed to establishing a quantitative understanding of the void-softening mechanism in shear. This information will be used to guide alloy design to achieve low shear banding propensity.

The key to understanding how microscopic voids deteriorate a plastically deforming metal is knowledge of the void region stress/ strain elevation over the uniform levels that would exist

in the absence of voids. Particularly useful would be knowledge of the void region state when the remote uniform field simulates the deformation occuring in a band of localized flow. This is the analytical problem addressed here. A set of elastic-plastic finite element analyses has been conducted to establish the local field between a pair of voids close enough to produce significant interactions.

The analyses were conducted using large scale computational facilities and an elastic-plastic finite element formulation for non-hardening Prandtl-Reuss constitutive theory[3]. The formulation is an incremental secant stiffness method that guarantees satisfaction of the yield condition at each grid point. An adaptive incrementation scheme is employed to automate load step size selection and to control load path discretization error. The formulation traces the spread of plasticity by adjusting element stiffnesses as the imposed displacement is incrementally increased. The mesh used to model the void pair in a plane strain deformation band is shown in Figure 1. There are approximately 1500 nodes (3000 degrees of freedom) in the mesh drawn. However, symmetry allows half of the model in simple shear analysis and a quadrant for uniaxial extension. All four sides of the band were constrained according to nominal deformation mode. In simple shear, the edges were constrained against vertical displacement, while in uniaxial extension, nodes on all four edges were constrained against horizontal motion. Thus, in the absence of the voids, the solutions would be uniform shear (no normal strain) and constant uniaxial extension (a single non-zero strain component).

The plastic zone development for the simple shear case is illustrated in Figure 2. In the early stages of loading, plastic deformation is restricted to regions at the void surfaces, roughly 45 degrees from the ligament. As these surface zones develop, a separate distinct plastic zone develops along the ligament. Once the zones link, plastic strain localization occurs between the voids. Figure 3 illustrates the fact that over the early stages of loading, straining is fairly uniform over the interior of the

14

ligament, but a maximum is seen to develop at a distance of 0.3 D ahead of the voids. The value of the maximum local shear strain is plotted versus nominal strain in Figure 4. The rate of increase of local strain with respect to applied strain continually rises with the final intensification rate in excess of thirty.

The plasticity and interaction for the case of uniaxial extension is much different than the above simple shear case. The plastic zone at a uniaxial strain value 1.27 Y/E is shown in Figure 5. Also shown in Figure 5 is that portion of the plastic zone that satisfies the near isocloric condition that the magnitude of the normal strain increments differ by less than 6%. Plasticity spreads from the void surfaces and excessive strain intensification occurs once the zones merge. The numerical data agrees with the logarithmic spiral distribution expected from slipline theory, Figure 7. Consistent with the plastic zone development, the maximum strain in this loading case is seen to occur at the void surfaces. The very significant intensification of strain suggests that substantial void growth will occur, in agreement with known results for the growth of isolated voids in triaxial stress fields[4].

In summary, the plasticity results for the test cases studied are consistent with experimental observations of void sheet development in shear and void growth in tension. Further work is being pursued to establish interaction features over a range of particle distribution parameters. The results suggest that the goal of establishing alloy development guidelines to minimize shear banding propensity using micromechanics is achievable and likely to be very worthwhile.

REFERENCES

1. J. A. Van Den Avyle, " Correlation of Fractography, Microstructure, and Fracture Toughness Behavior of High Strength Alloys," Ph.D. Thesis, MIT, Cambridge, MA, 1975.

2. M. Azrin, J. Cowie, and G. Olsen, private communication, Army Materials Technology Laboratory, 1986.

3. D. M. Tracey and C. E. Freese, "Adaptive Load Incrementation in Elastic-Plastic Finite Element Analysis," Computers and Structures, 13, pp. 45-53, 1981.

4. J. R. Rice and D. M. Tracey, "The Ductile Enlargement of Voids in Triaxial Stress Fields," J. Mechs. Phys. Solids, 17, pp. 201-207, 1969.
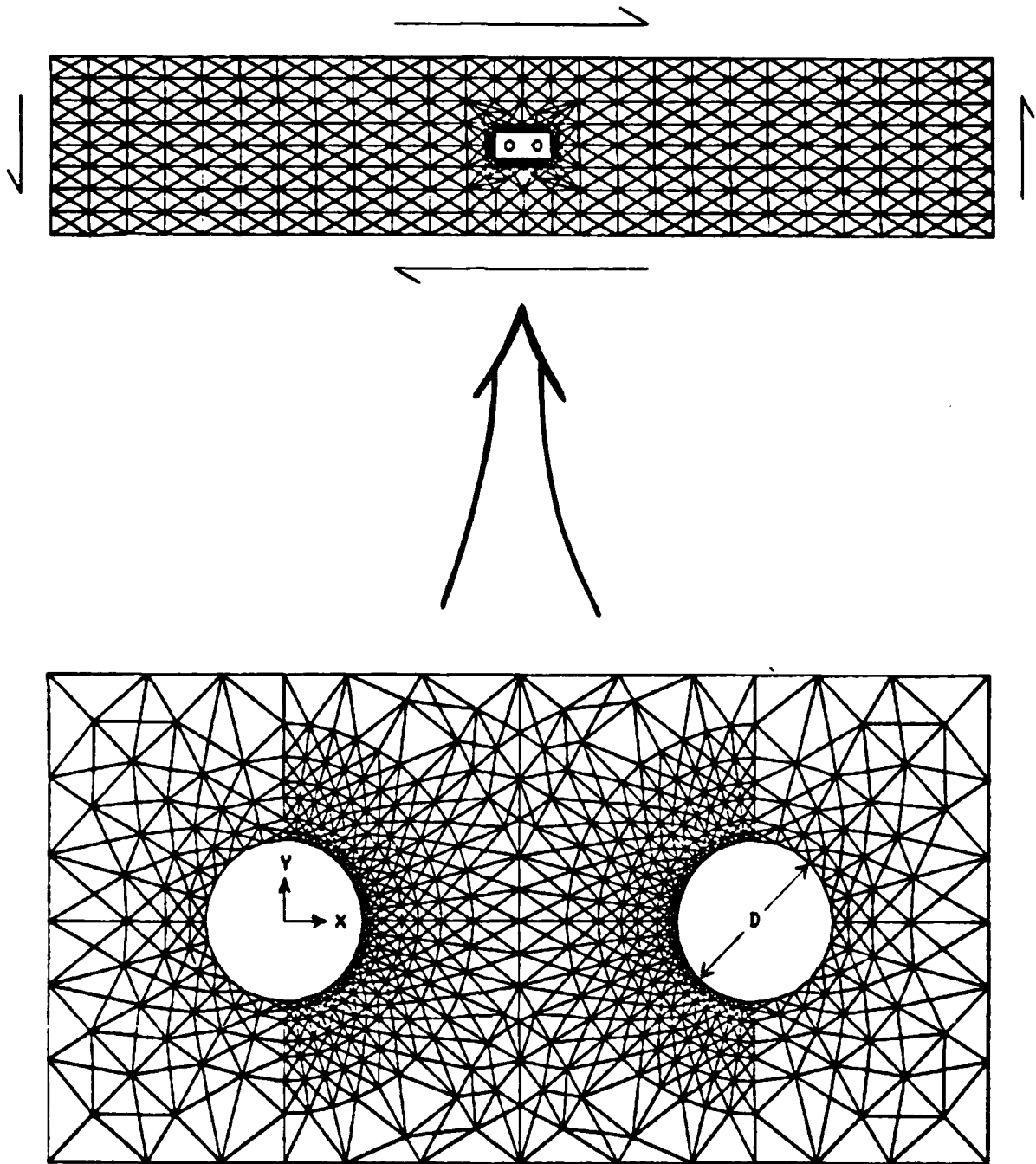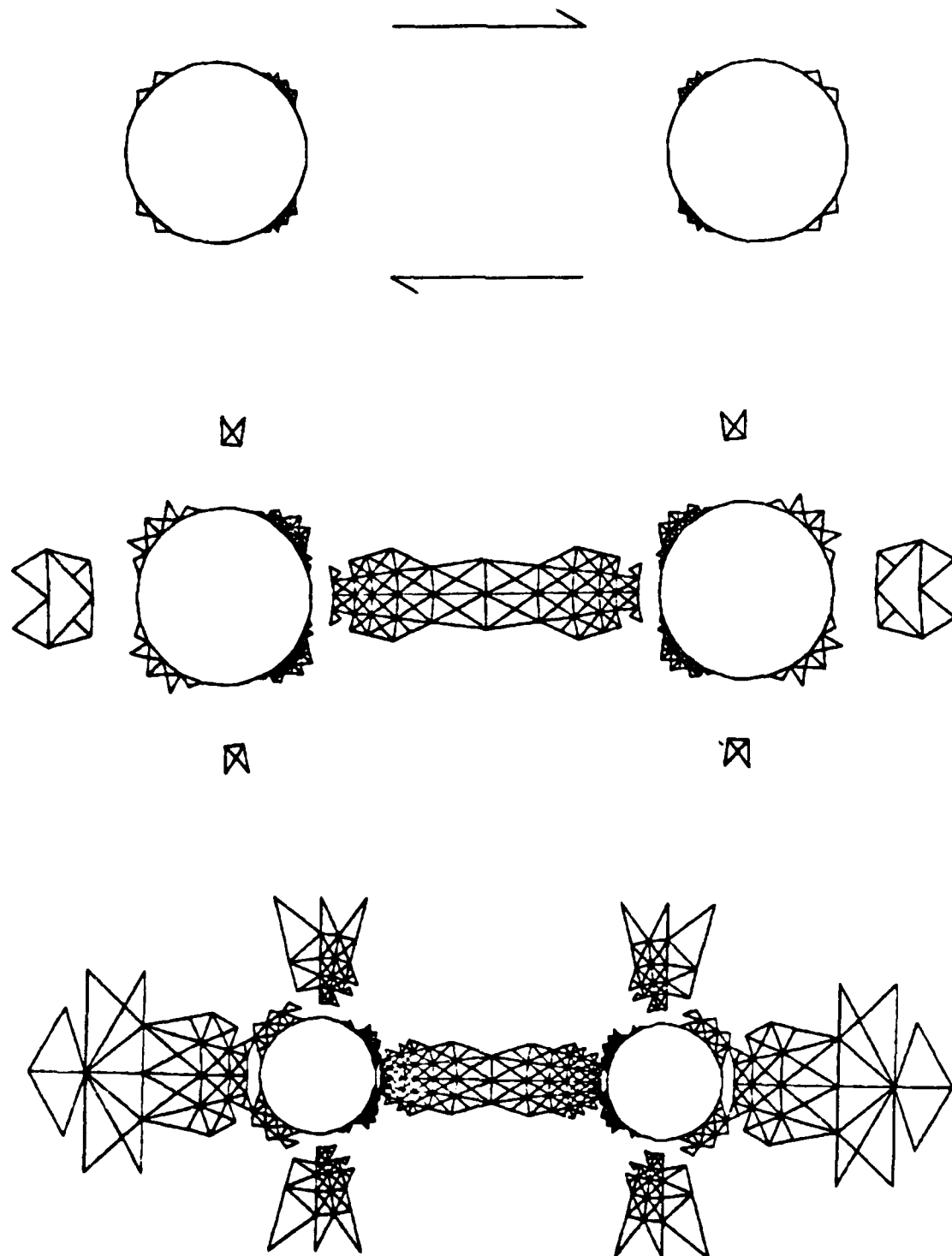
FIGURE 1 - Pair of voids in deformation band

FIGURE 2 - Development of plastic instability between void pair under simple shear. Plastic zones at nominal shear strain levels 60, 77, and 91% of γ_{yield}
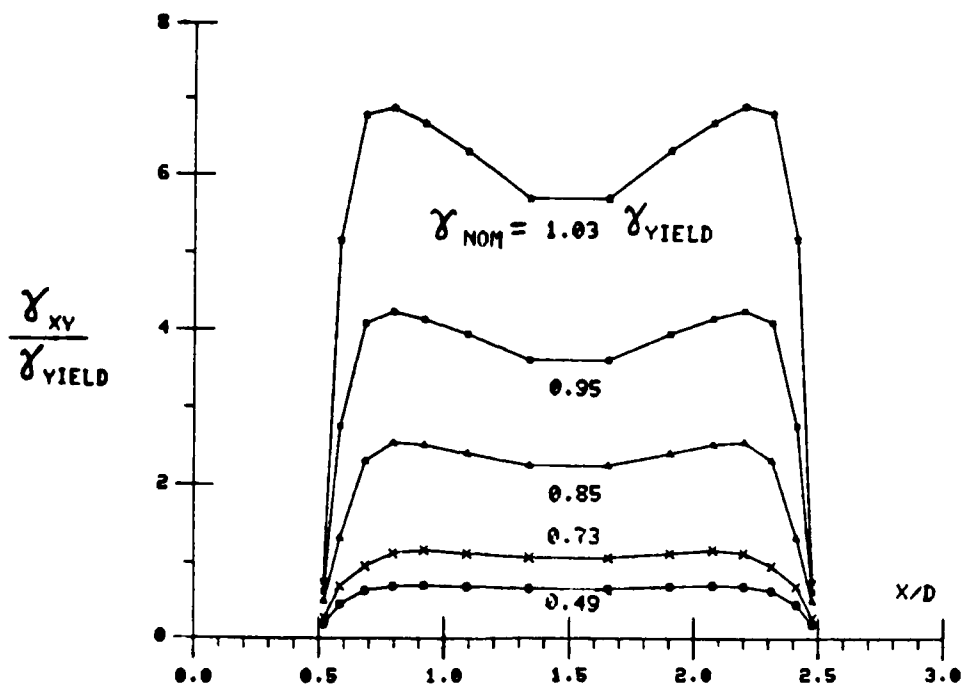
FIGURE 3 – Shear strain distributions on ligament between voids under nominal simple shear
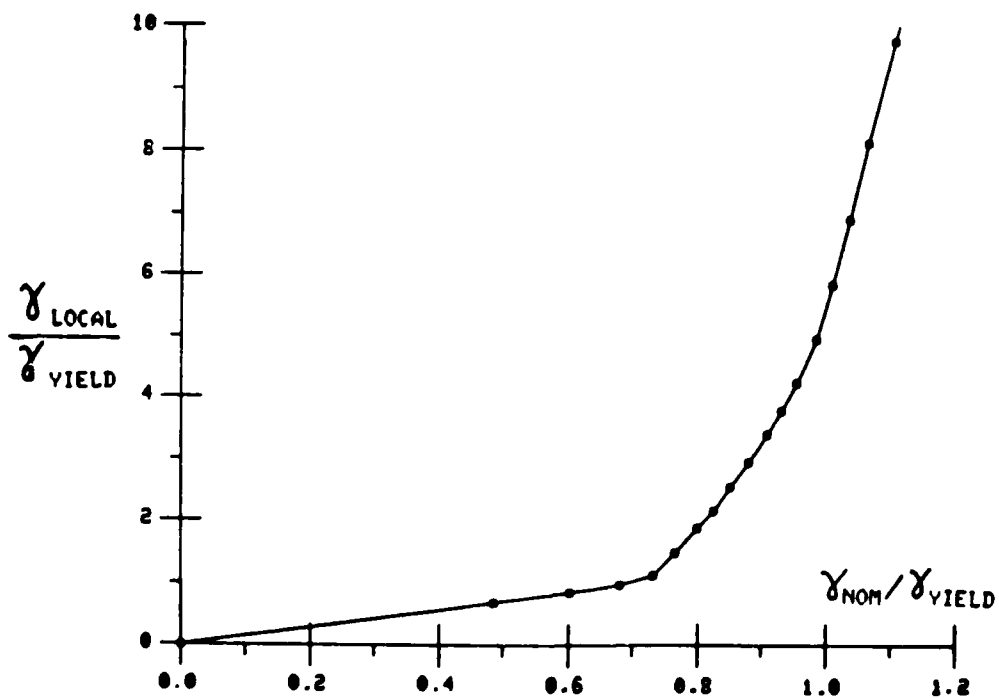
FIGURE 4 – Strain intensification between voids under nominal simple shear

19

$\epsilon_{\text{NOM}} = 1.27 \ Y/E$

(A)

$\beta = .06$

(B)

FIGURE 5 - (A) Plastic zone under nominal uniaxial strain
level 1.27 Y/E
(B) Fully developed near-isocloric portion of
plastic zone shown in (A)

FIGURE 6 - Numerical data for normal stress on ligament at
nominal uniaxial strain 1.27 Y/E compared with
slipline theory logarithmic spiral distribution

FIGURE 7 - Normal strain distribution on ligament between
voids under nominal uniaxial strain

21

A Study of the Crack Tip Parameters that Govern Environmentally Assisted Cracking by Use of the Rising Displacement Test
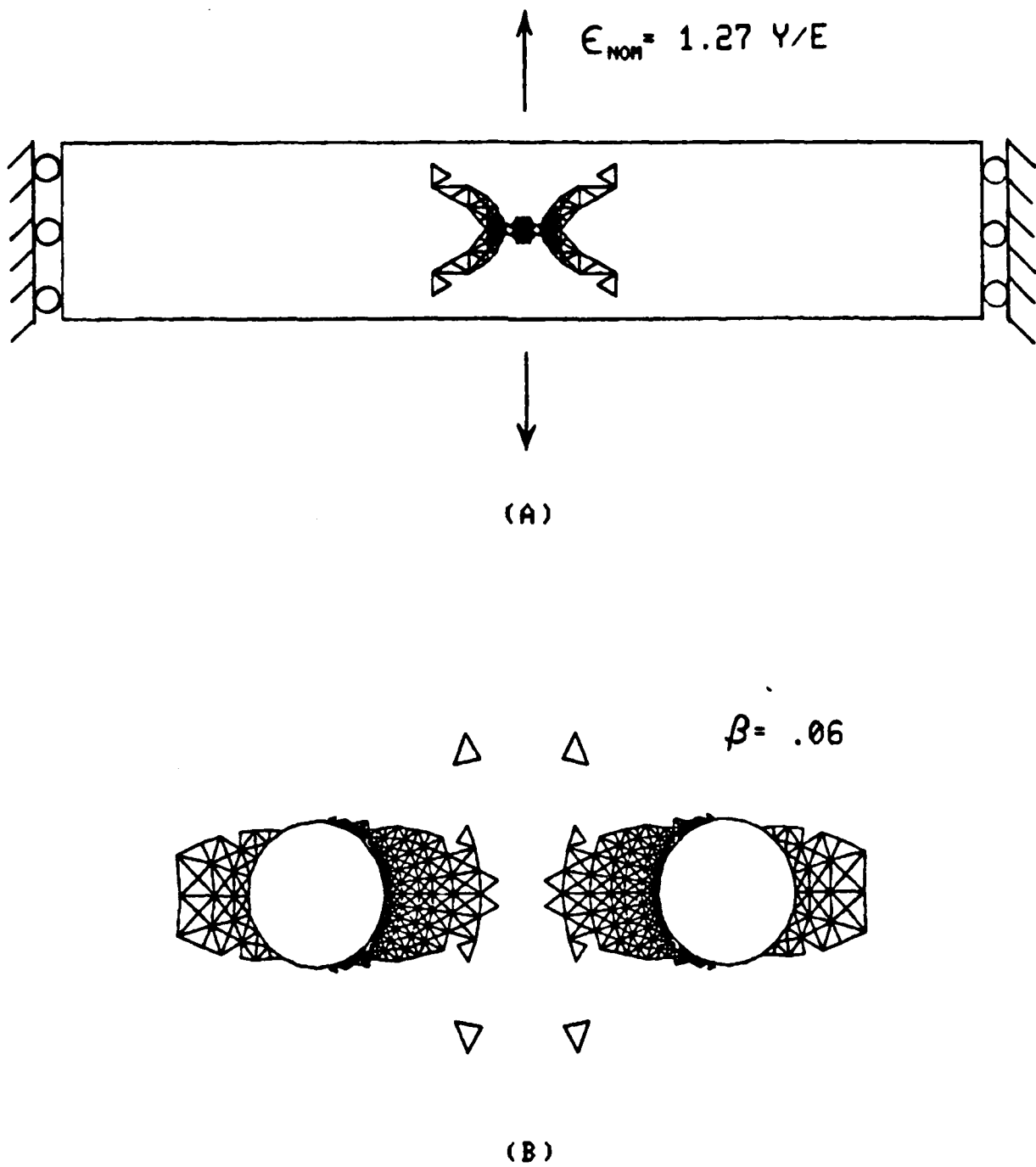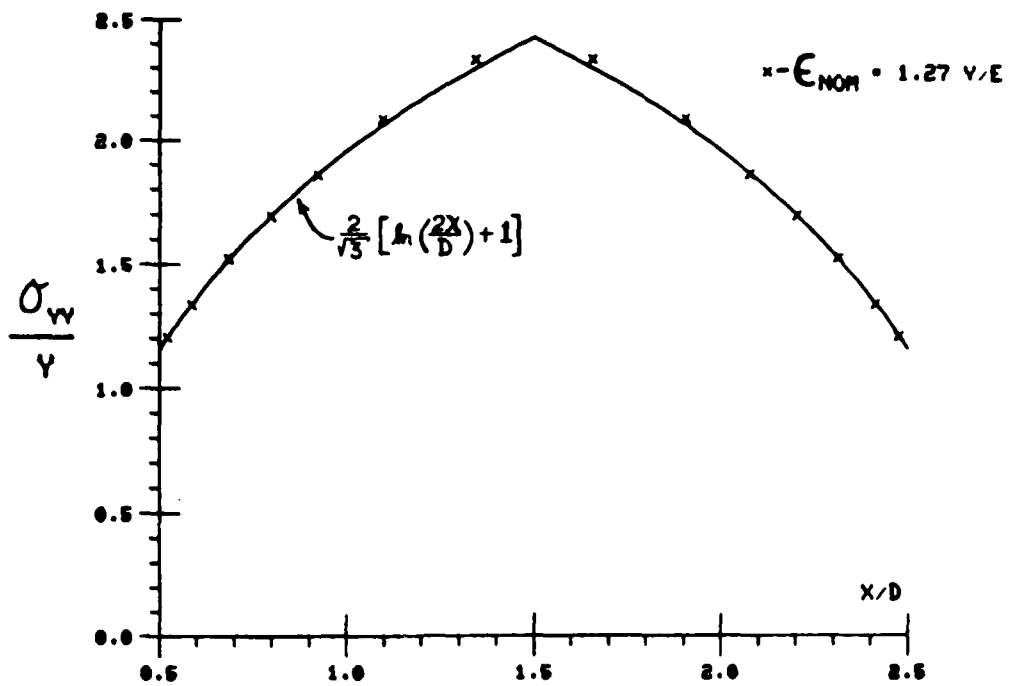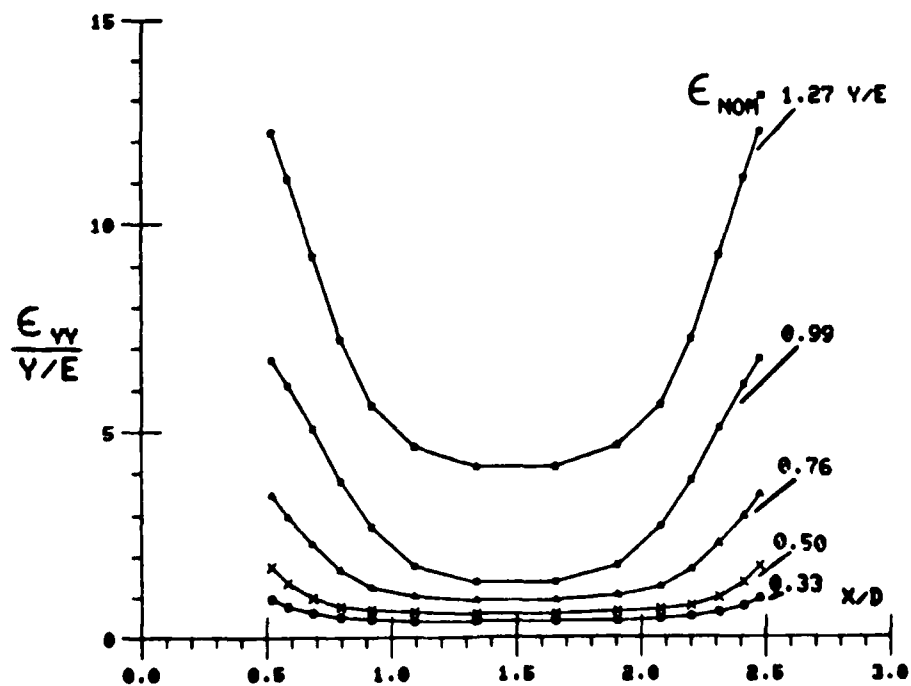
by

R. Mayville, T. Warren and P. Hilton
A.D. Little, Inc., Cambridge, MA

Abstract

There is an increasing interest in the use of rising displacement or load tests, similar to K-R or J-R resistance curve tests, to characterize environmentally assisted cracking (EAC) in metal/environment systems. These tests have been used to determine K_{IEAC} (K_{ISCC}) and to study the effect that crack tip parameters, such as K_I, dJ/dt and $d\delta/dt$, have on EAC. This investigation is an experimental study of the effect a wide range of applied displacement rates has on EAC for AISI 4340 with $\sigma_o = 1095$ MPa (159 ksi) in flowing synthetic seawater. Cantilever beam - constant load - tests were performed to obtain $K_{IEAC} = 98$ MPa $\sqrt{m}$. Rising displacement tests were performed over four orders of magnitude with 25mm thick compact tension specimens under ambient conditions and in environment to generate J-R curves and to determine crack velocities. Under ambient conditions the 4340 exhibits substantial stable tearing. In environment, the J-R curves were identical to the ambient J-R curve except for the slowest test, which lasted over a week. The J-R curve for this specimen was substantially lower than the ambient curve and K_{IJ} converted from J_{IC} was found to agree very well with K_{IEAC}. The J-R curves are shown in Figure 1. Two experiments were also performed in environment in which the displacement - stroke - was held constant after some stable crack extension had occurred. The crack velocities from these and the other compact tension tests are plotted in Figure 2 against K_I and indicate that the $\dot{a}$-K_I relationship is unique for environmental cracking for $K_I > K_{IJ}$ (from ambient J_{iC}). In addition, the environmental $\dot{a}$-K_I curve is

parallel to the ambient $\dot{a}$-K_I curve suggesting that the ambient mechanical cracking mechanisms play a major role in environmental cracking for this system. This is supported by very similar ductile rupture fracture surfaces for the two cases. This work has been supported by the National Science Foundation and by the Arthur D. Little Corporate Fund.

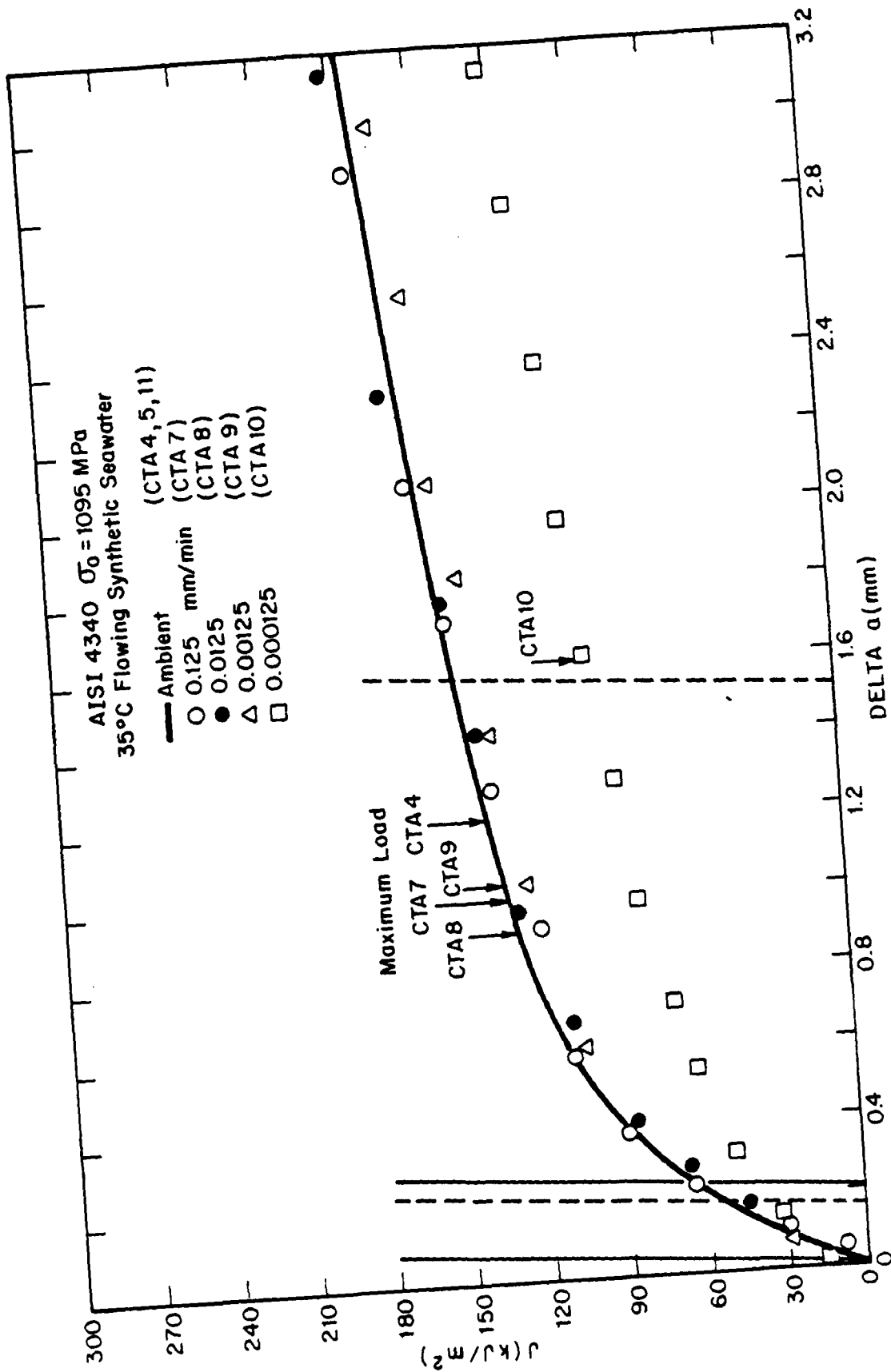Key words for Army Symposium: fracture mechanics, experimental methods, life prediction.

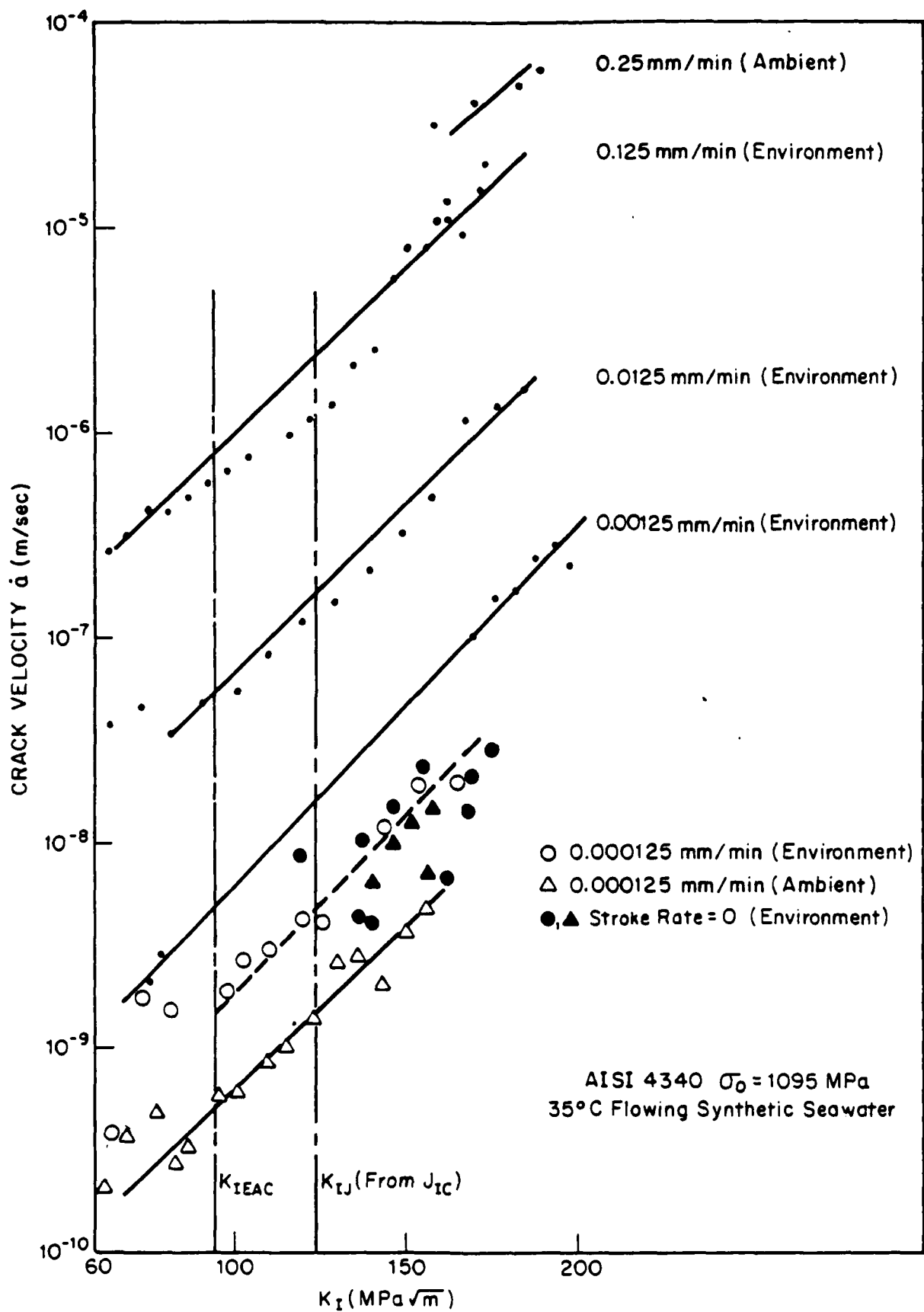Figure 1: J-R Curves in Environment at Four Displacement Rates in Comparison to the Ambient J-R Curve

25

Figure 2: Crack Velocity Data from the Compact Tension Specimens

EXPLICIT AND IMPLICIT SOIL MODELLING FOR DYNAMIC SOIL-STRUCTURE INTERACTION PROBLEMS

Aaron Das Gupta, Ph.D.
US Army Ballistic Research Laboratory
Aberdeen Proving Ground, Maryland 21005-5066

ABSTRACT

Increased application of nonlinear viscoelastic materials in structures and consideration of operating environments require modeling of interaction of such structures with the surrounding soil medium which significantly influences the dynamic response when subjected to an impulse or blast over-pressure loading. The need is currently accentuated by the rapid advances in numerical modeling of dynamic problems using either finite-difference or finite element techniques of structural analysis.

While various models are available to describe the deformation and failure processes, scarcity of dynamic experimental data at high strain rates is a serious handicap for a majority of representative soil materials. As a result, many computations are still made using static or low strain rate data. In order to overcome this critical shortcoming in soil-structure inter-action problems, an explicit modeling technique could be improvised by representing the soil with an equivalent mechanical model consisting of a spring and a dashpot in parallel and connecting the model to the structural model using node-tie element. In this spring support condition, the base of a structure in contact with soil could be flexibly supported using an appropriate value of the spring stiffness while the top of the structure could be loaded directly.

The implicit modeling technique where nodal tie elements are used to model the base support as nonlinear springs for shallow buried structures to simulate the soil medium suffers from a serious shortcoming in sofaras the indirect loading of the structure through shock waves passing through the soil and overpressure loading attenuation effects are not adequately modeled resulting in unrealistic soil-structure interaction and erroneous results. Hence an explicit modeling technique is recommended whereby a few layers of soil surrounding the base of the structure are modeled as an assembly of elements in contact with the structure. The interfacing cantact elements for both structure and soil are allowed to stick, slide or seperate from each other to simulate the appropriate boundary condi-tions.

The explicit modeling technique using a finite element code require characterization of constitutive relationship of geological materials from shock compression behavior of such materials and their Hugoniot charac-teristics. Although the equations-of-state in the form of pressure-density relationships for shock propagation in such mediums can be non-linear, the characterization technique in this investigation is currently restricted to materials with linear Hugoniot characteristics at all pressure ranges.

Three representative soil mediums i.e., saturated and unsaturated tuff, oil shale and sand are selected for this study. Under the assumption of unidimensional shock propagation and conservation law of mass, momentum and energy, the equations-of-state could be transformed to bulk moduli versus volumetric strain relationship using the methodology described in this paper. The transformed characterization is compatible with the tension cutoff curve description material model available in the ADINA nonlinear dynamic finite element analysis program. However, the characterization of sand is valid in this study only at very high pressure regimes where sand behaves like quartz due to solid phase transition and a linear Hugoniot curve fit to the shock velocity versus particle velocity data is feasible.

The method could be readily extended to partially saturated soil with nonlinear characteristics through multilinear approximation during the loading and unloading phase. The resulting constitutive relationship will facilitate explicit modeling of the surrounding medium around shallow-buried structures and realistic simulation of dynamic soil-structure interaction which can significantly alter the dynamic response behavior of such structures.

ABSTRACT

COMPOSITE MATERIALS APPLICATIONS PROGRAM

AT THE US ARMY BALLISTIC RESEARCH LABORATORY

WORK IN PROGRESS

RICHARD B. MURRAY
Mechanical Engineer
Mechanics and Structures Branch
US Army Ballistic Research Lab

EDWARD M. PATTON
Team Leader, Material Applications
Mechanics and Structures Branch
US Army Ballistic Research Lab

LARRY W. BURTON
Mechanical Engineer
Mechanics and Structures Branch
US Army Ballistic Research Lab

ROBERT P. KASTE
Mechanical Engineer
Mechanics and Structures Branch
US Army Ballistic Research Lab

EXTENDED ABSTRACT

The Mechanics and Structures Branch of the Interior Ballistics Division of the
Ballistic Research Laboratory has embarked upon a mission program tailored to
understanding composite materials and their potential application to Army
systems. The intent of the program is to provide the Army with design techniques
and prediction methodologies specifically aimed at the problems peculiar to Army
systems. These problems include high rates of loading, including ballistic
loadings and blast loadings; high and low cycle fatigue; corrosion and erosion
resistance; and the necessity to predict structural response of thick sections to
all loading environments. The intent is also to attempt to apply new and
emerging materials developed at other Army laboratories, under other Army
programs, and those materials available in the commercial sector. The approach
to this broad scoped and general program has been to decide which issues are the
most important to the designers of some specific systems and components, and
initially concentrate upon those aspects of the material systems which are not
yet well understood. Three of these aspects of composite material behavior have
been selected as the most critical current predictive techniques for composite
materials. They are : structural response to high rates of loading, predicting
structural response of thick sections of laid-up laminated structures, and
failure criteria for thick laminates. The remainder of this abstract will focus
on the work in progress in these three critical areas.

HIGH RATE LOADING

We are developing an instrumented projectile that can be launched from a 37mm gun housed in an indoor range at BRL. This gun/projectile system can be used to ballistically test a sample encased within the instrumented projectile. By changing the charge and/or mass and/or geometry of the projectile, a wide range of ballistic loading rates and states of stress of interest can be investigated. It is intended that samples of composite materials will be made up and loaded in the instrumented projectile for tests. Data such as strain and strain rate in several directions and at several locations within the sample will be taken. These data will then be correlated with finite element structural simulations of the tests to determine the efficacy of a particular modelling method, and also to benchmark that method. In this way, predictive techniques of structural response at the rates of loading of interest can be developed and benchmarked before being applied to full scale Army systems and components.

THICK SECTIONS

Army structural components tend, in general, to be larger, thicker, and more massive than do structural components for agencies such as the Air Force or NASA. The major studies to date that have been performed, and a majority of the structures which have manufactured have been for those two agencies. These structures tend to be two dimensional curved or cylindrical structures with or without stiffening ribs. Army Structures, such as howitzer components and armored vehicle hulls, tend to be made of thick, strong, massive components. To date, very little analytical work has been performed for this type of structure.

A major portion of the composite material application program has had to deal with just this problem. How does one predict structural response of a thick laminated section. Laminated plate theory fairly accurately predicts the response of thin structural components such as wing skins or rocket motor housings, but the theory fails to accurately predict the response of thick laminates. We have therefore taken a broad approach to attacking this problem. First, several experts from within and outside of the Army laboratories have been contacted. Experts from two of the pre-eminent centers for composites have been brought under contract to derive failure criteria. This will be discussed later in this abstract.

Secondly, a small laboratory is being set up which is specifically geared toward constructing samples of thick sections for testing. Both an injection molding machine and a small autoclave will be used to make up test samples of thick sections for mechanical testing and benchmarking of structural predictive techniques.

FAILURE CRITERIA

All of the structural response predictions that can be made are worthless unless we can predict whether or not the structure survives its loading environment. One of the most important parts of this program is, therefore, the prediction of failure, and the criteria whereby that failure is predicted. There are many schools of thought concerning failure prediction in laminated structures. There are almost as many as there are experts predicting the failure. They can, however, be broken into two general categories; maximum stress criteria and maximum strain criteria. Experts from both the Air Force Materials Lab and Lawrence Livermore Laboratories are working under contract on one or the other of these general criteria. It is intended that the results of these two studies will be integrated into a design tool for use by Army systems designers which will allow these designers to accurately predict the response and failure of structural components. Enough intelligence will be built into this predictive tool to allow the designer to select from several approaches to laying up a laminate, and several approaches to predicting the response and/or failure of the component in question.

CLOSURE

We have embarked on a long term and intentionally aggressive program for the development of predictive techniques and design methodologies for application of composite materials to Army structural components and systems. The program has elements of pure research into predictive techniques for thick sections and failure of components, and elements of experimental work in high rates of loading common to Army Ballistic comonents. The program has a very broad scope, but is focused upon the peculiar needs of Army component and systems designers. It meshes well with ongoing programs at other major Army laboratories in composite materials development, and it also has brought together a large body of knowledge from outside experts in an effort to capitalize on as much of the present knowledge and technology of composite materials as possible.

31

EFFECTIVE TREATMENT OF MEMBRANE AND SHEAR LOCKING PHENOMENA IN CURVED SHEAR-DEFORMABLE AXISYMMETRIC SHELL ELEMENT

A. Tessler and L. Spiridigliozzi
U.S. Army Materials Technology Laboratory
Watertown, Massachusetts 02172

Wide varieties of structural shells exhibit geometric and material symmetry. As such, they are best modeled by appropriate shell of revolution finite elements which are intrinsically one-dimensional. Thus, computationally efficient analyses are possible owing to the small bandwidth and dramatically reduced number of degrees-of-freedom, as compared to the alternative discretizations with more 'expensive' two-dimensional shell elements.

Design requirements for thin and moderately thick shells and in particular those made of laminated organic composite materials necessitate accurate modeling of the shell geometry and proper account of the effects due to shear deformation and, in dynamics, rotary inertia. To be effective, therefore, an element should be able to accommodate these higher-order effects and closely approximate the meridian curvature. Additionally, nodal simplicity is commonly desired, especially if computationally involved nonlinear analyses are warranted.

A major difficulty intrinsic to shear-deformable bending elements is due to a mathematical deficiency called 'shear locking'; (the term refers to nearly trivial kinematic patterns manifested in the thin regime due to an overly stiff model). A mathematically analogous phenomenon known as 'membrane locking' is a common hindrance in curved bending elements. Thus, formulating a curved shear-deformable element requires simultaneous resolution of the two locking phenomena.

In this paper we present a simple, yet extremely effective, two-node, displacement-type, axisymmetric shell element derived from Naghdi's refined shell theory [1] with the aid of the Marguerre shallowness equations [2]. This work is an extension of the conical shell element discussed in [3] and the Timoshenko-Marguerre beam [4]. Here, we adopt the anisoparametric kinematic approximations which employ distinctly different degree polynomials for the kinematic variables, rather than uniform interpolations as in the conventional isoparametric procedure. Owing to these approximations, both the membrane and shear strains, which serve as penalty constraints in the thin-element regime, possess physically admissible penalty modes. The formulation is further enhanced by an innovative treatment of the two penalty parameters (nondimensional multipliers of the shear and membrane strain energies), giving rise to the appropriate relaxation of the penalty straining for coarsely discretized models. To focus on the core issues, only the axisymmetric response of linearly elastic isotropic shells is considered; note that extensions to asymmetric response and laminated composites are straightforward once the 'locking issues' have been conceptually resolved.

The main features of this two-node, six degrees-of-freedom shell element are summarized as follows (refer to Fig. 1 for the shell notation):

1. The meridian variation of the element geometric description is taken as cubic and is given in terms of two nodal slopes β_0 and β_1, which are assumed to be small (i.e., the geometry is shallow in the Marguerre sense).

2. The kinematic variables u (membrane displacement), w (transverse displacement) and θ (cross-sectional rotation about the normal to the meridian) are interpolated in the meridian direction by quartic, quadratic and linear polynomials , respectively. The quartic u is coupled in terms of u_i, w_i, and θ_i (i=0,1) degrees-of-freedom; the quadratic w is coupled in terms of w_i and θ_i degrees-of-freedom; and the linear θ is solely dependent upon its nodal values θ_i. In the particular case of a straight meridian, u reduces to an independent linear function in terms of u_i degrees-of-freedom.

3. Because of the specific choice of the kinematic approximations, the membrane strain, bending curvature and shear strain acting in the meridian direction are constant. Thus, only one-point Gaussian quadrature is needed to integrate the corresponding strain energies exactly.

4. Element stiffness and consistent mass matrices, and consistent load vector are derived via Hamilton's variational principle where full Guassian quadratures are employed on all energy terms.

5. The shear and membrane relaxation parameters depend exclusively upon element geometric and material properties and yield a well-conditioned stiffness matrix for any shell thickness. Importantly, these relaxation measures give rise to notable accuracy enhancements in coarsely discretized models.

Numerical studies are carried out focusing on the element modeling capabilities in free vibration problems.
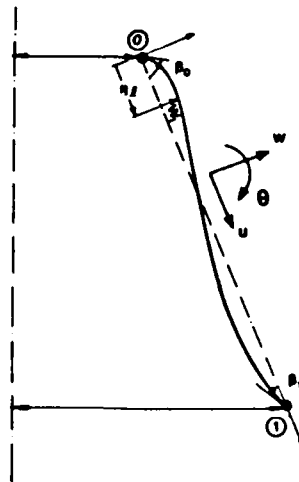

Fig. 1. Shallowly curved axisymmetric shell element.

REFERENCES

1. Naghdi, P.M. "Foundation of elastic theory", in Progress in Solid Mechanics, (eds. I.N. Sneddon and R. Hill), North-Holland, Amsterdam, Vol. IV, Chap. 1, 1963.

2. Marguerre, K. "Zur Theorie der gekrummten Platte grosser Fomenderung", Proc. 5th Internat. Congress of Applied Mechanics, 693-701, 1938.

3. Tessler, A. "An efficient, conforming axisymmetric shell element including transverse shear and rotary inertia", Computers and Structures, 15, 567-574, 1982.

4. Tessler, A. and Spiridigliozzi, L. "Curved beam elements with penalty relaxation", to appear in Internat. J. Numer. Meth. Engrg. (1986).

PLANE STRAIN FINITE ELEMENT ANALYSIS OF
RUBBER TRACK PADS

A. R. Johnson and C. J. Quigley
United States Army Laboratory Command
Army Materials Technology Laboratory
Watertown, MA 02172-0001

EXTENDED ABSTRACT

Rubber track pads used on Army tanks are subjected to large loads. The loading environment consists of repeated compression loads applied by the road wheels, penetration by rocks or metal debris, scuffing and cutting. Failure modes include chunking, subsurface cracking and blowout from hysteretic heating. It is not practical to try and model all possible loading situations to which a track pad may be exposed. Instead, to screen new material candidates, laboratory tests and analyses of samples can be made. These tests and analyses should subject the material to the various modes of loading expected so that materials which perform better than the current standard can be identified.

During the past two years MTL has started a research program to develop finite element analysis capabilities for determining the large deformations and stresses in elastomer (rubber) materials used in vehicles. The finite element programs developed can be used to analyze and design the laboratory tests mentioned above. In this effort[1] a total Lagrangian potential energy formulation with a Valanis-Landel[1] form for an energy density function was used to model elastomers. A nonlinear finite element algorithm was developed which used bilinear three node triangular elements to minimize the potential energy. Elastomer cylinders loaded in both end thrust and by a probe along the cylinder axis were analyzed[2,3,4]. More recently, a modified form[5] of the classical Mooney-Rivlin energy density functional was derived[5] which allows for computation of rubber deformations without the hydrostatic pressure as an independent variable. Also, a quadratic six node finite element formulation has been developed[6].

The analyses of axisymmetric deformations of rubber[2-6] can be modified to allow for the computation of plane strain rubber deformations. In this effort we show the plane strain formulation and present numerical data obtained for a two dimensional model of an Army T-156 track pad. The notation used to describe the stretching of the material is shown in Figure 1. Both three node bilinear and six node biquadratic elements are shown in Figure 2. One half of a finite element model for a T-156 track pad is shown in Figure 3. The energy density functions used are as follows:

VALANIS-LANDEL

$$w = 2\mu \sum_{i=1}^{3} \lambda_i(\ln\lambda_i - 1) + \frac{1}{2}\hat{\lambda}[\ln(\lambda_1\lambda_2\lambda_3)]^2$$

MODIFIED MOONEY-RIVLIN

$$w = c_1(I-3K^{1/3}) + c_2(J-3K^{2/3}) + \frac{1}{2}\hat{\lambda}\ln^2 K$$

where w = energy per unit undeformed body,

λ_i = the i'th stretch ratio,

$I = \lambda_1^2+\lambda_2^2+\lambda_3^2$,

$J = \lambda_1^2\lambda_2^2+\lambda_2^2\lambda_3^2+\lambda_3^2\lambda_1^2$,

$K = \lambda_1^2\lambda_2^2\lambda_3^2$,

$\mu, \hat{\lambda}$ = the Lamé constants,

and c_1, c_2 = material coefficients from classical Mooney-Rivlin energy density functional.

REFERENCES

1. K. C. Valanis and R. F. Landel, "The strain energy function of a hyperelastic material in terms of the extension ratios", J. of Applied Physics, Vol. 38, No. 7, June 1967, 2997 -3002.

2. A. R. Johnson, C. J. Quigley and I. Fried, "Large Deformations of elastomer cylinders subjected to end thrust and probe penetration", Third Army Conf. on Applied Math. and Computing, Georgia Inst. Tech., Atlanta, Georgia, 1985.

3. A. R. Johnson, C. J. Quigley and I. Fried, "Stretching in an elastomer cylinder during an axial probe penetration", Thirty-Second Sagamore Army Materials Research Conference, Lake Luzerne, NY, July 1985.

4. A. R. Johnson, C. J. Quigley and I. Fried, "Computer modeling of solid elastomer cylinders used in material performance tests", US Army Survivable Tire Symposium 85, Ormsby House, Carson City, Nevada, November 1985.

5. I. Fried, A. R. Johnson and C. J. Quigley, "Admissible Elastic Energy Density Functions for Rubber-Like Solids", Fourth Army Conference on Applied Mathematics and Computing, Cornell University, May 1986.

6. I. Fried and A. R. Johnson, "Nonlinear computation of axisymmetric solid rubber deformation", submitted to Computer Methods in Applied Mechanics and Engineering.

undeformed   deformed
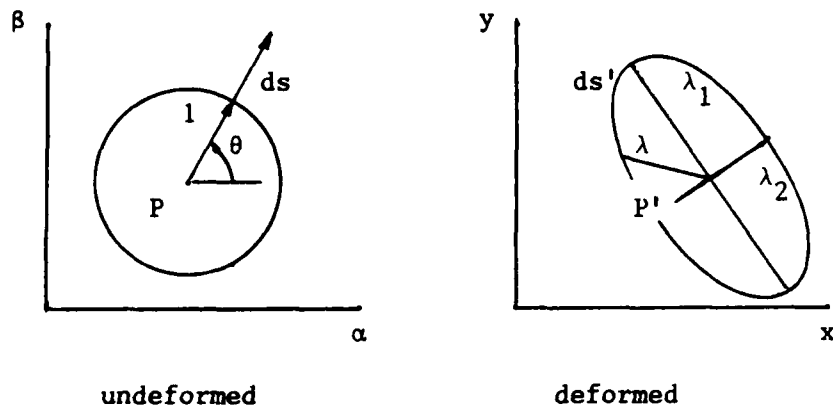
$$\lambda^2(\theta) = (\frac{ds'}{ds})^2$$

Find

$$\lambda_1^2 = \frac{1}{2}[a+b+[(a-b)^2+4c^2]^{1/2}]$$

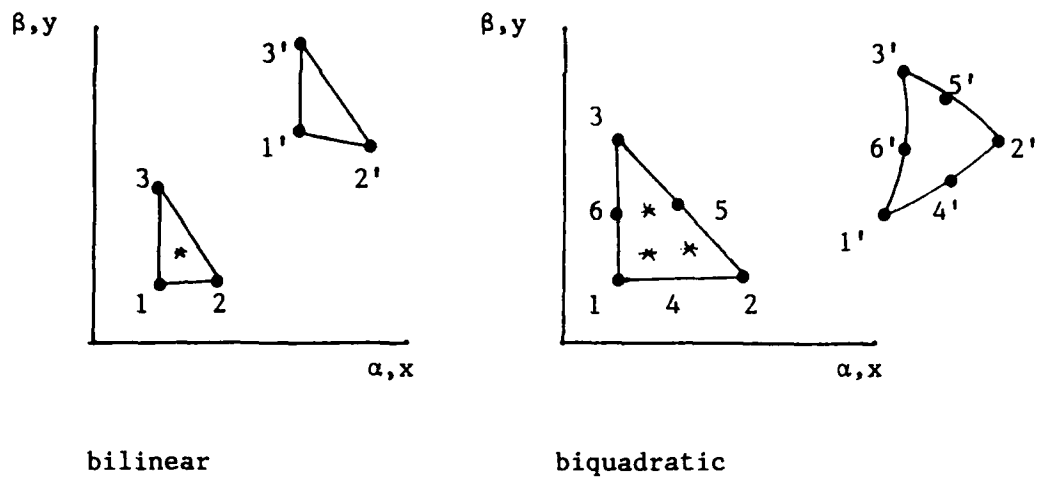$$\lambda_2^2 = \frac{1}{2}[a+b-[(a-b)^2+4c^2]^{1/2}]$$

$$\lambda_3 = 1$$

where

$$a = x_{,\alpha}^2 + y_{,\alpha}^2$$

$$b = x_{,\beta}^2 + y_{,\beta}^2$$

$$c = x_{,\alpha}x_{,\beta} + y_{,\alpha}y_{,\beta}$$

Figure 1. Description of material line deformation and stretch ratios.

bilinear   biquadratic

* = integration point.

Figure 2.   Bilinear and biquadratic elements used to discretize the
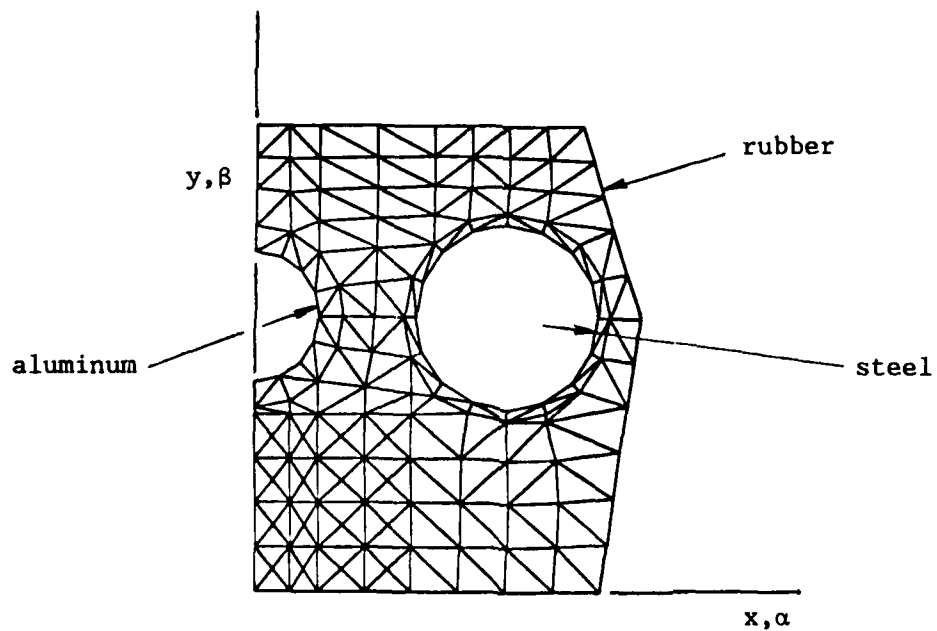   potential energy.

Figure 3.   Plane strain T-156 tank track pad finite element model.

ANALYSIS AND TESTING OF PREDAMAGED SHELL STRUCTURES

Richard E. Keeffe
Sr. Research Scientist
Kaman Sciences Corp.
Colo Spgs, Colo 80907

Eric Reece
Member Technical Staff
Sandia National Laboratories
Albuquerque, New Mexico 87185

EXTENDED ABSTRACT

A predamaged shell structure may undergo significant reduction in load carrying capacity, dependent upon the location, size, and shape of the damaged area. Kaman Sciences Corporation[1] (KSC) and Sandia National Labs (SNLA) under direction from the U.S. Army Strategic Defense Command are investigating analytic and experimental methods for evaluation of these effects. This paper reviews some results of work in progress and planned structural test efforts aimed at supplying data for analytic correlations.

Of primary concern are thin walled cylindrical and conical shell frustra which have locally damaged areas as indicated in Figure 1. Note that these damages are idealized and that in general, damages may be irregular in nature. As shown, three basic loading conditions are of interest.

1. Axial Tension
2. Axial Compresison
3. Lateral Bending

Note that two bending configurations will be studied; one with the damaged area in tension, the second with the damaged area in compression.
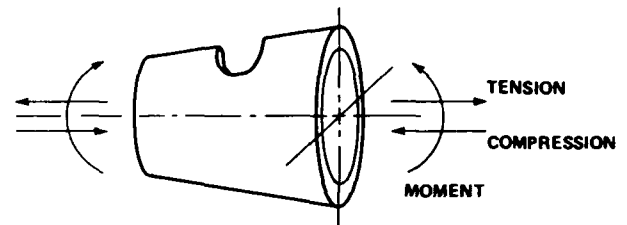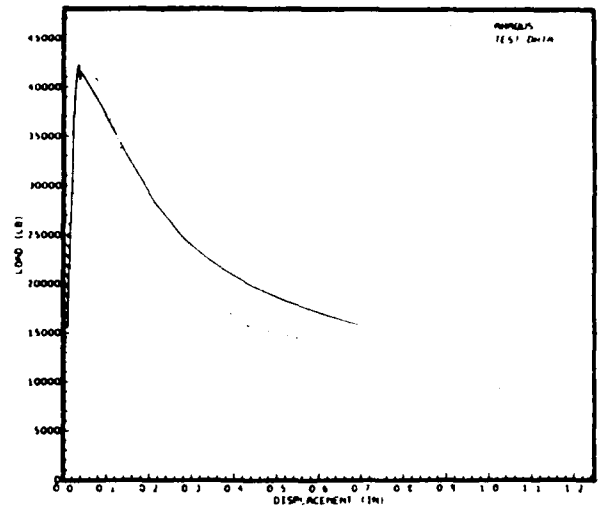

FIGURE 1
DAMAGED SHELL GEOMETRY

The basic analysis tool currently being considered for these studies involves application of the nonlinear finite element code ABAQUS, developed and maintained by HIBBITT, KARLSSON and SORENSON, INC. The code capabilities include static and dynamic modeling of solid, beam, and shell elements, and provides accurate modeling for arbitrary magnitudes of displacement, rotation, and strain. Preliminary assessment of the applicability of the ABAQUS formulation has been applied to tension and compression test results obtained on 6061-T6 seamless aluminum cylinders[2]. Slot damages were machined in one

---

(1) This work is being performed under Contract DASG60-85-C-0051 for the USASDC Huntsville, Alabama. Mr. Owen Bender (USASDC) is the contract monitor.

(2) This Testing was performed at Southwest Research Institute, San Antonio, Texas under subcontract to Kaman Sciences Corporation.

side of these cylinders and compression and
tension tests (with clamped ends) were
performed to large deformation and frac-
ture. Axial load vs total axial deflection
predicted using ABAQUS are compared to test
results in Figure 2. The comparison shown
was obtained using an initial radial
imperfection of .01 inches (.254 mm) at the
shell midplane. Additional variations in
initial imperfections are being analyzed.
The final deformed mesh geometry (X2.5)
predicted by ABACUS is presented in Figure
3(a), along with a photograph of the post
test shell specimen (Figure 3b). In
general the comparisons between test and
theory are promising for this single shell
geometry.

FIGURE 2
ANALYSIS TEST COMPARISON

(a)

(b)
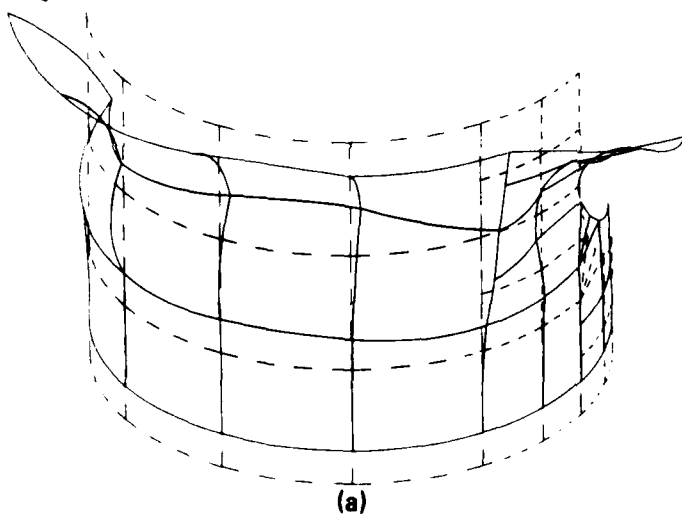
FIGURE 3
SHELL DEFORMATION

A more ambitious combined analysis and test program involving two layered
conical frustra is currently underway. Table I presents a conical frustra
test matrix planned for FY 1986-87. The initial tests will incorporate
single, circular hole damage patterns. Additional tests planned for 1987 will
include multiple hole patterns and non circular damages. Actual testing will
be performed by the Sandia National Laboratories in Albuquerque, New Mexico.

42

TABLE I
CONICAL FRUSTRA TEST MATRIX

TEST TYPE	DAMAGE* LEVEL	NUMBER OF TESTS FOR EACH DAMAGE HOLE TYPE			NUMBER OF HOLES	TEST DATE	
		CIRCULAR	SIMULATED	IRREGULAR		FY86	FY87
AXIAL TENSION	15%	1			1		1
	25%	1			1	1	
	25%	1			2		1
	15-25%		1	1	1		2
	25%		1	1	2		2
	35%		1	1	1		2
AXIAL COMPRESSION	15%	1			1		1
	25%	3			1	3	
	25%	1			2		1
	15-25%		1	1	1		2
	25%		1	1	2		2
	35%		1	1	1		2
BENDING (DAMAGE HOLE IN TENSION)	15%	1			1		1
	25%	1			1		1
	25%	1			2		1
	35%	1			1		1
	15-25%		1	1	1		2
	25%		1	1	2		2
	35%		1	1	1		2
BENDING (DAMAGE HOLE IN COM-PRESSION)	15%	1			1		1
	25%	1			1		1
	25%	1			2		1
	35%	1			1		1
	15-25%		1	1	1		2
	25%		1	1	2		2
	35%		1	1	1		2
					TEST SUBTOTALS	4	36

* Max Circumferential Removal

43

CORROSION CONTROL BY COMPOSITE MATERIAL SUBSTITUTION WITH APPLICATION TO THE M-939 5 TON TRUCK

PIN TONG, Chief Structures and Dynamics Division
TRANSPORTATION SYSTEMS CENTER
CAMBRIDGE, MA 02142

In an effort to improve the corrosion resistance of the 5-ton M-939 truck and to lighten its weight, the Army is evaluating the replacement of structural components which have high potential for environmental deterioration with equivalent composite components. As a part of this overall effort, several graphite epoxy chassis were fabricated by Ewald Associates. A schematic of the chassis is shown in figure 1. These chassis were designed to match the strength and stiffness characterisitcs of the steel chassis and weigh about 50% less. One of the chassis has been installed in an actual truck and is being used for demonstration purposes.

The present study involves the evaluation of the prototype chassis both as fabricated and as installed in the 5-ton truck for corrosion resistance, structural integrity, and damage tolerance. Of interest is the sensitivity of the composite frame mechanical details to stress concentrations, fracture, shock and vibration and environmently produced degradation particularly from moisture and abrasion. Additionally, other structural components which are critically sensitive to corrosion and may afford a great weight saving potential will be identified and alternative composite designs developed. Finally, a prototype truck employing as many light weight corrosion resistant components as possible will be designed, fabricated, and tested.

In the initial phase of this project a methodology has been developed to evaluate the composite frames. This methodology involves identifying stress sensitive locations, characterizing static strength and dynamic flexibility of the composite frame, and evaluating the in service stresses. The first step has been to compare the stiffness characteristics, as well as the first bending and warping natural frequencies of the composite frame with the steel frame. In addition, the worst case loading conditions have been identified and a simple dynamic model proposed. Estimates are developed for the effect of the assembly modifications made to the Ewald frame currently installed in an actual truck.

Test plans for the truck with the composite chassis include estimating the principle connection stiffness and damping characteristics of an assembled truck. These parameters are required for the dynamic model of the truck in conjuction with road spectrum data, for the prediction of life cycle estimates. Of critical concern is the potential for environmental deterioration of the frame especially at or near the mechanical fasteners. Tests conducted on coupons or sample mechanical details are planned to evaluate effects such as moisture content and operating temperature ($-25^{\circ}F$ to $+125^{\circ}F$). These tests will include sensitivity to freeze-thaw cycles and mechanical abrasion.

Numerous truck components have been identified as corrosion sensitive with some potential for weight reduction, also, designs for these components will be developed and evaluated for structural capacity, particularly in reference to abrasion, environmental deterioration, and damage tolerance. The final phase of the project will be the fabrication, assembly and service testing of a prototype truck encompassing all the light weight corrosion resistant components developed.
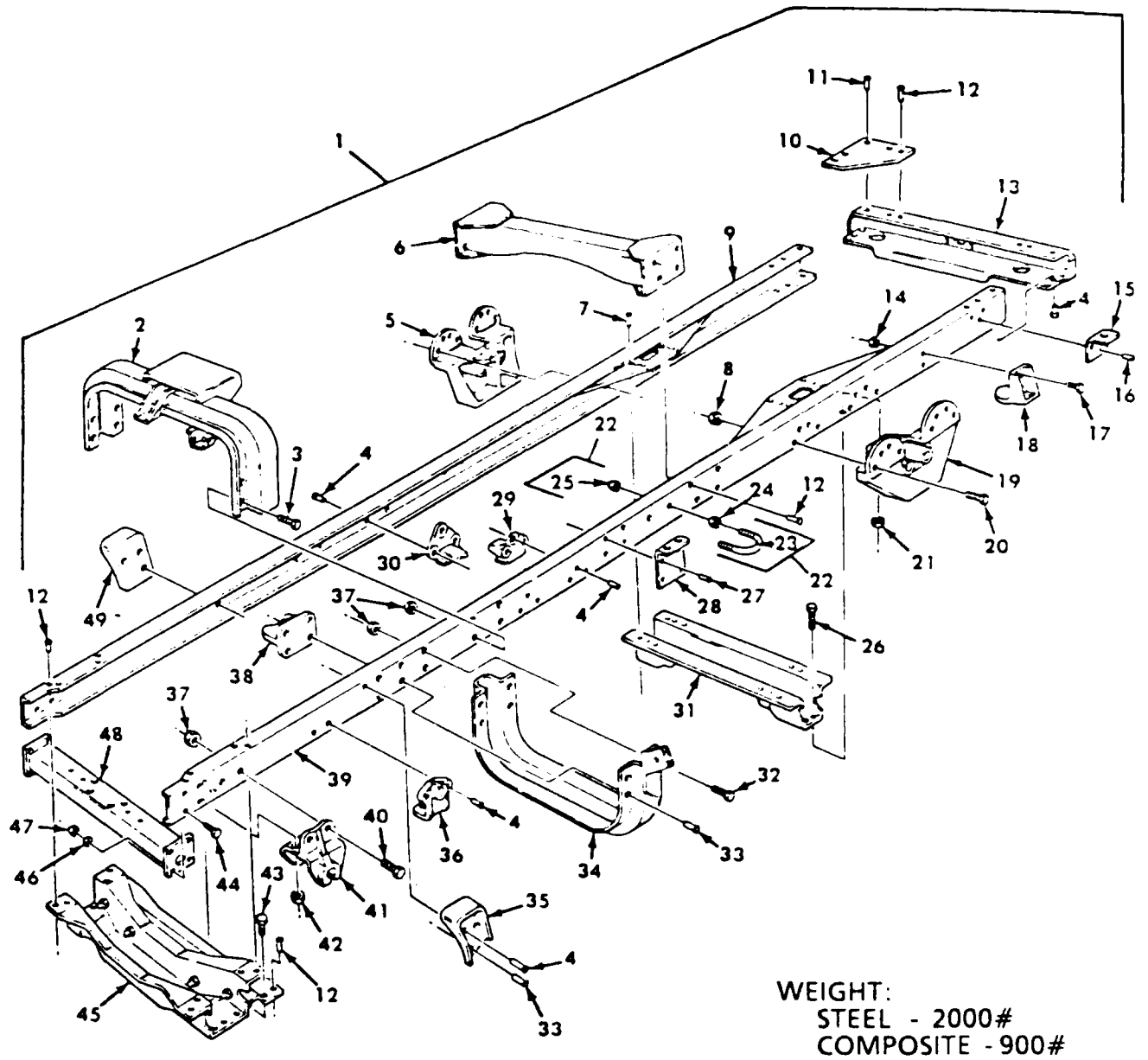
WEIGHT:
STEEL - 2000#
COMPOSITE - 900#

Figure 1. CURRENT STEEL 5-TON TRUCK CHASSIS

Durability of Powdered Aluminum Structures

by

Karen Severyns
Margery Artley
Air Force Wright Aeronautical Laboratories
AFWAL/FIBEC
WPAFB, Ohio 45433

Many high strength, low density powdered metals are being developed for aerospace applications. Advantages in mechanical properties, such as lower density, higher fracture. toughness, and much higher strength, in powdered metallurgy wrought products are due to the fine grain structure resulting from rapid solidification achieved by powder atomization. Powdered metallurgy (P/M) offers signficant improvements in material properties over ingot metallurgy (I/M).

Although the physical and mechanical properties of P/M materials are still being quantified, properties of P/M alloys are promising greater load-carrying capability and/or reduced weight in high-stress, fracture critical airframe applications. Even with this promising outlook, the applicabilty of powdered metals in fracture critical aerospace components is uncertain. In order to help maximize the performance of military aircraft, this research program is being conducted to investigate the crack growth characteristics of a representative powdered aluminum, and to characterize the initial quality and fatigue crack growth rates of P/M aluminum for durability and damage tolerance analysis. In addition to determining if traditional crack growth fracture mechanics analysis is possible, this program will ensure that structures made of P/M aluminum can be designed to ensure structural integrity.

This research program investigates the characteristic properties of extruded bar stock 7091 T7E69, a first generation, high strength P/M aluminum produced by ALCOA. The test specimens of dimensions 4"x.5"x48" have several different flaw geometries including elox center starter notches of approximately .1" (figure 1A), open holes 0.25" in diameter (figure 1B), open holes 0.25" in diameter with corner flaws (figure 1C), and open holes 0.25" in diameter with thru-the-thickness flaws (figure 1D). The flaw geometries were prepared sixteen inches (16") apart to ensure no load interaction between the two holes or notches.

The test plan includes four tensile tests to determine the mechanical properties of 7091, and ninety-four fatigue crack growth tests of constant amplitude and variable amplitude load histories. The variable amplitude load history being used is a programmed F-16 load history containing predominately tension-tension cycles as well as a few compression cycles with each block representing 400 flight hours.

To date, all tensile tests and twenty-five fatigue tests have been completed. The fatigue test specimens show extreme out of plane cracking and tunneling (figure 2). Believing that the out of plane crack growth was due to the thickness of the specimen (.5") and residual surface stresses, the specimens were modified. In an attempt to alleviate surface stresses and to control the non-planar crack growth, the specimens were milled to 3.9"x.4"x48". Then the maximum stress level was reduced from 30 KSI to 25 KSI. In the thinner specimens, the crack growth rate decreases, and the total life is increased by twenty six blocks on the average. Also the angle, θ, at which the crack deviates from the plane of the flaw is decreased by forty percent on the average (figure 3). The thinner specimens appear to exhibit better crack growth, yet this crack growth still exhibits extreme non-planar growth and tunneling.

The fatigue crack growth of P/M 7091 is extremely consistent. The characteristic nature of non-planar crack growth and tunneling is present in all of the fatigue test specimens. The non-planar crack growth and tunneling is not dependent on the thickness of the specimen or the maximum stress level. For this reason, it is believed that the non-planar crack growth is completely normal for P/M 7091 and that linear elastic fracture mechanics may not apply to P/M metals. A new method must be developed to analyze the fatigue crack growth of P/M 7091 and all other P/M metals.

Tensile tests showed that P/M 7091 demonstrates an average yield strength of 72.7 KSI, an average ultimate strength of 83.9 KSI, and an average modulus of elasticity of 9.9×10^6 PSI. I/M 7075 T7 demonstrates a yield strength of 59 KSI, an ultimate strength of 80 KSI, and a modulus of elasticity of 10.4×10^6 PSI. Therefore P/M 7091 has an improved yield strength and ultimate strength over I/M 7075, but a decreased modulus of elasticity.

Before any more fatigue testing is performed, life predictions will be developed for P/M 7091 using the Walker equation. Then testing will be resumed to check the accuracy of the developed equation. Adjustments to the equation will be made if necessary.

Conclusions of this research on the durability of powdered aluminum structures will be documented when the fatigue test program is completed.
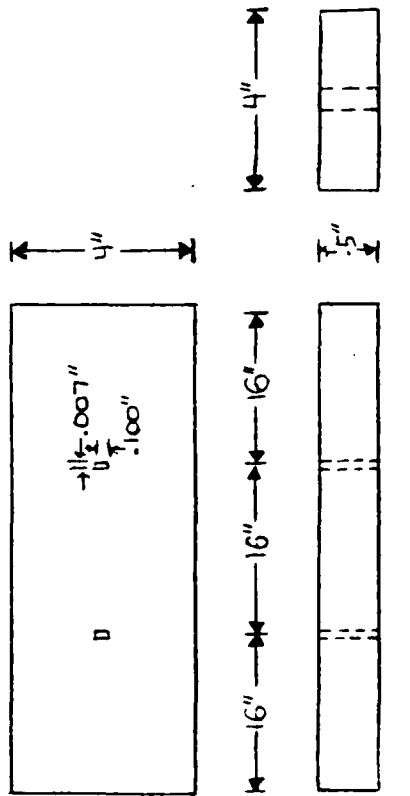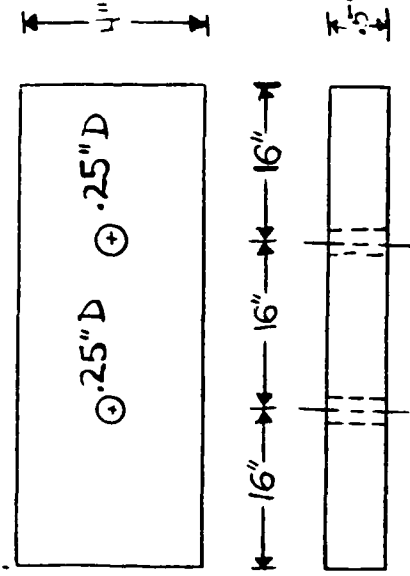
NOTE: NOT TO SCALE

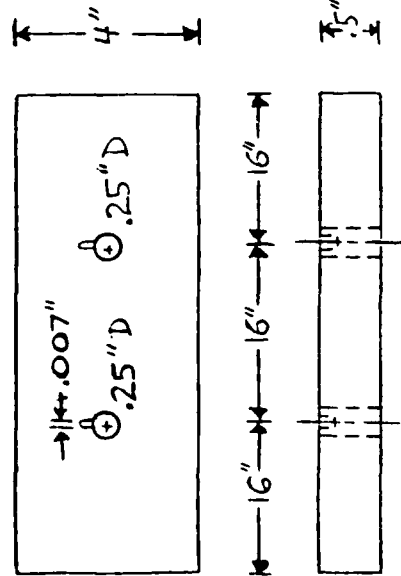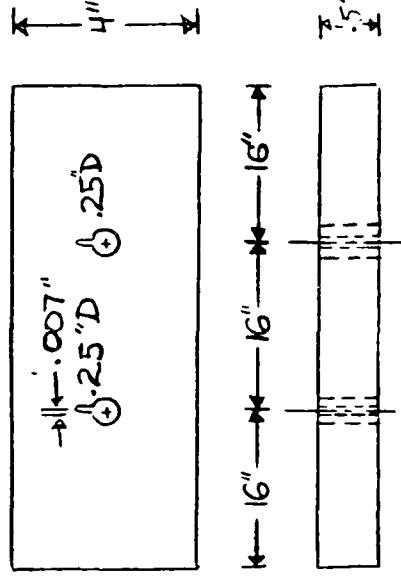
Figure 1A

Figure 1B

Figure 1C

Figure 1D

Figure 1:
A.) Geometry of the elox slot specimen
B.) Geometry of the unflawed hole specimen
C.) Geometry of the corner flaw specimen
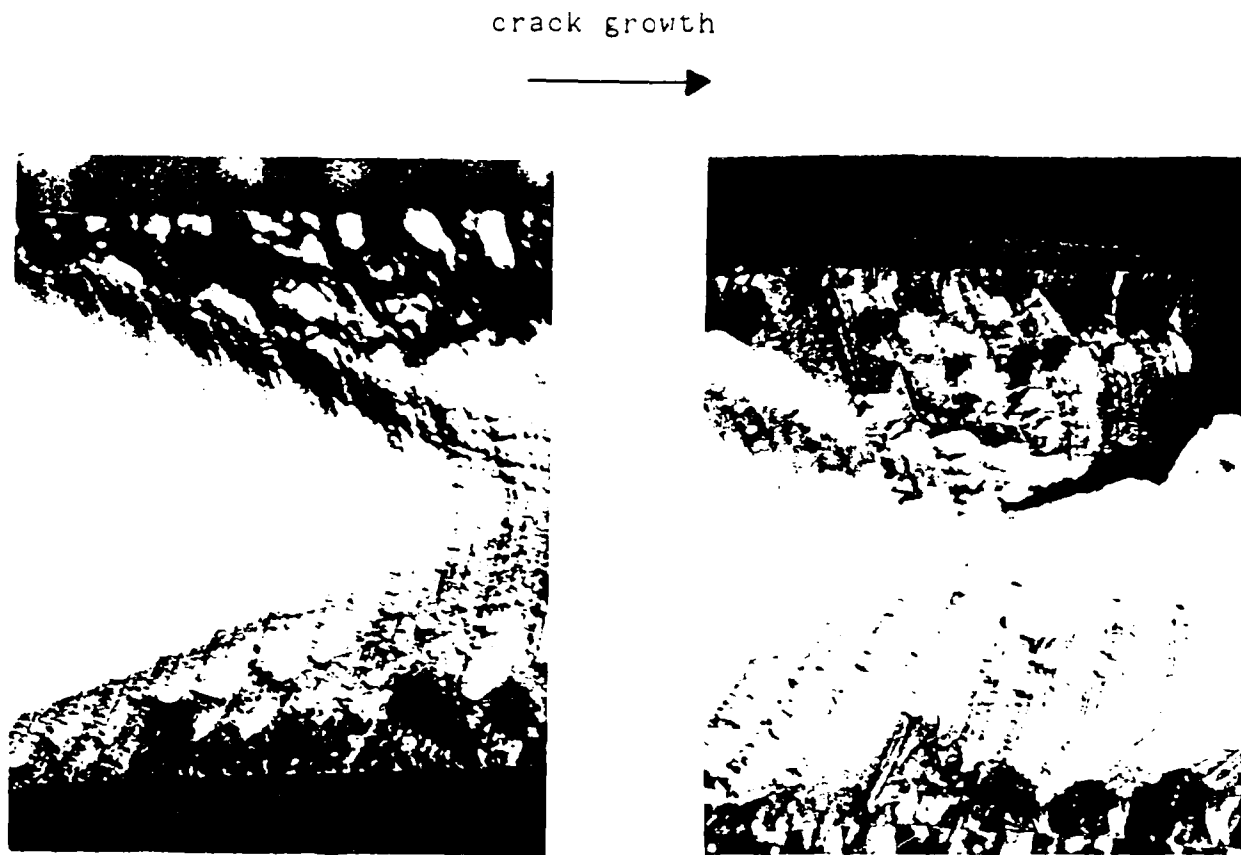D.) Geometry of the thru-the-thickness specimen

51

crack growth ⟶

Figure 2: Fracture surface of P/M 7091

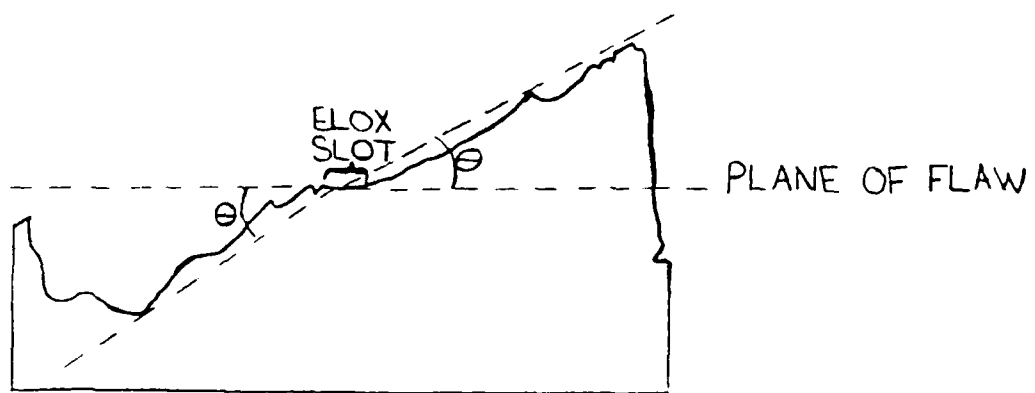Figure 3: Θ, angle at which the crack deviates from the
plane of the flaw

Some Mechanics Considerations in Ceramic Gun Barrel Liners*

R. Barsoum, P. Perrone, P. Wong
U.S. Army Materials Technology Laboratory
Watertown, MA

E. Bunning
SACO Defense, Inc.
SACO, ME 04072

The problem of erosion and wear of gun barrels has long been recognized. Ceramic materials offer the most favorable combination of high hardness, compressive strength, erosion resistance and chemical inertness at high temperature. In recognition of the potential of ceramics for gun barrel life improvement, MTL and DARPA contracted with SACO Defense Systems Division to investigate the feasibility of a ceramic-lined barrel.

This work-in-progress report describes the analysis and failure evaluations of the tests performed on three potential ceramic liner materials. The ceramic lined gun barrel test assembly is shown in Figure 1. The ceramic liners have an interference fit. They are assembled by a shrink fitting process first to the steel sleeve, then to the steel jacket. Shrink fitting is performed in order to introduce favorable compressive stress in the ceramic, which could negate any tensile stresses arising during firing. Finally, the liner retainer and nozzle attachments are assembled. Following that the ceramic liner is thoroughly inspected using a boroscope before the firing tests. After each firing the ceramic liner is also inspected for any cracks.

The three ceramic materials tested were α-SiC, Si_3N_4 and PSZ/TS. Table 1 gives a summary of the firing test results and failure modes observed.

In order to understand the cause of failure in each case, a finite element analysis was performed. The finite element analysis attempted to simulate the shrink fit operations and firing conditions. It should be mentioned that SACO performed a Lame analysis in order to evaluate the interference fit and firing stresses. The finite element model in Figure 2 emphasized the details at muzzle end of the ceramic liner where most of the failures occurred.

Figures 3 to 8 show the hoop and axial stresses due to shrink fit and firing and are used in the failure analysis.

---

*This program is Co-sponsored by MTL and DARPA.

The presentation will discuss the analysis results for the assembly operation and firing. The failures observed of the three materials are correlated with the analysis results. It will also cover the use of the finite element results in a Weibull analysis to evaluate the probability of failures. Dynamic effects, design changes and recommendations for improved performance will be discussed also.

TABLE 1 – SUMMARY OF FIRING TEST RESULTS

| Material	Liner Config.	Shrinkfit Inside	Shrinkfit Outside	Rds. Fired	Failure Mode	Comments
α-SiC	Cylindr.	.002	.002	1000	None	No increase in bore dia.
α-SiC	Cylindr.	.003	.002	375	Circumferential crack at breech.	Removed circumferential crack at muzzle before test. Bore at breech oversize.
α-SiC	Cylindr.	.004	.002		Existing crack widened.	Circumferential crack at muzzle before shrink.
α-SiC	Tapered	.0017/.0002	.002	1	Axial crack	Insufficient interference
α-SiC	Tapered	.0035/.0024	.0021	6	Circumferential cracks at muzzle.	
α-SiC	Cylindr.	.0035	.002	16	Circumferential cracks at muzzle.	Circumferential crack at muzzle before test.
$Si_3 N_4$	Cylindr.	.0018	.0023	500	Axial cracks at muzzle end.	No increase in bore dia. Crack origin near muzzle?
$Si_3 N_4$	Cylindr.	.0018	.0023	1010	None	No increase in bore dia.
PSZ/TS?	Cylindr.	.002	.002	31	Circumferential cracks at muzzle.	Circumferential crack at muzzle before test.
PSZ/TS	Cylindr.	.002	.002	36	Surface flaking and cracks.	Thermal failure?
PSZ/TS	Cylindr.	.002	.002	246	Surface flaking and crack.	Thermal failure?

55
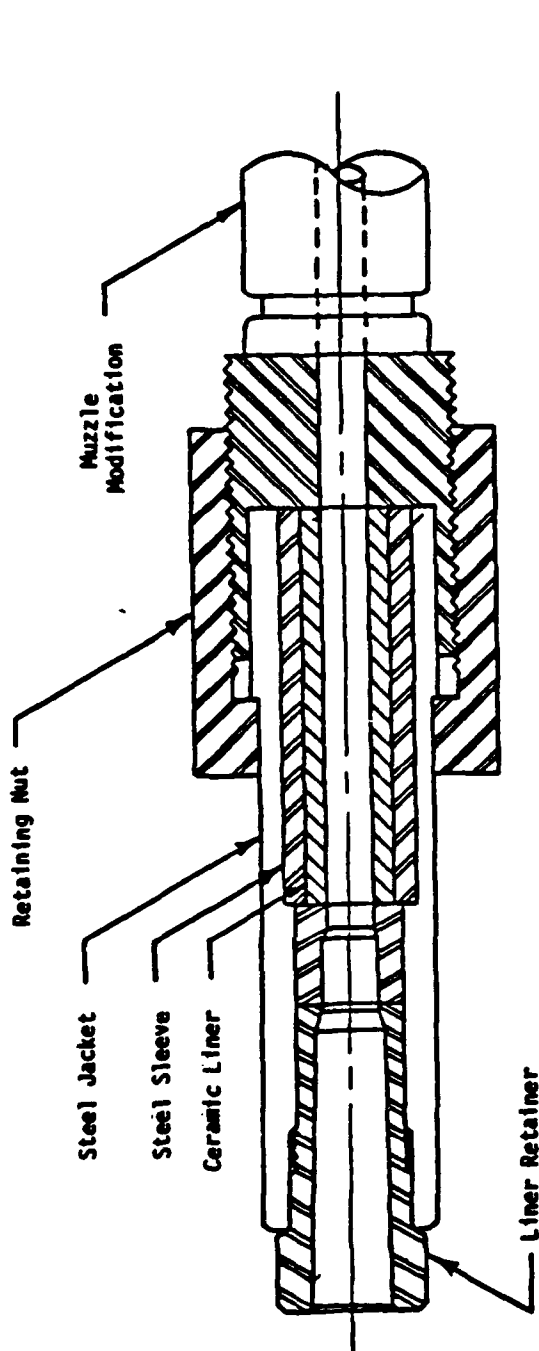
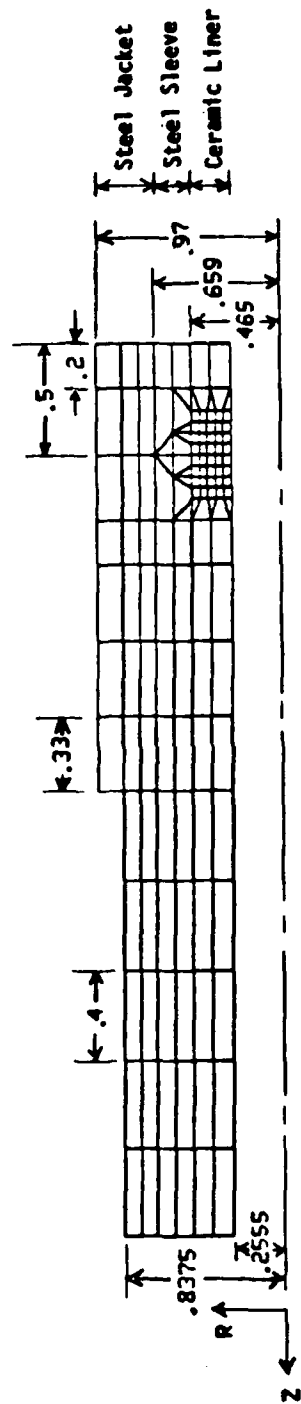FIGURE 1 – Schematic of ceramic lined gun barrel test assembly

FIGURE 2 – Finite element model of gun barrel section containing ceramic liner

56

FIGURE 4 – Contour plot of axial stress due to shrink fit and firing with an α-SiC liner
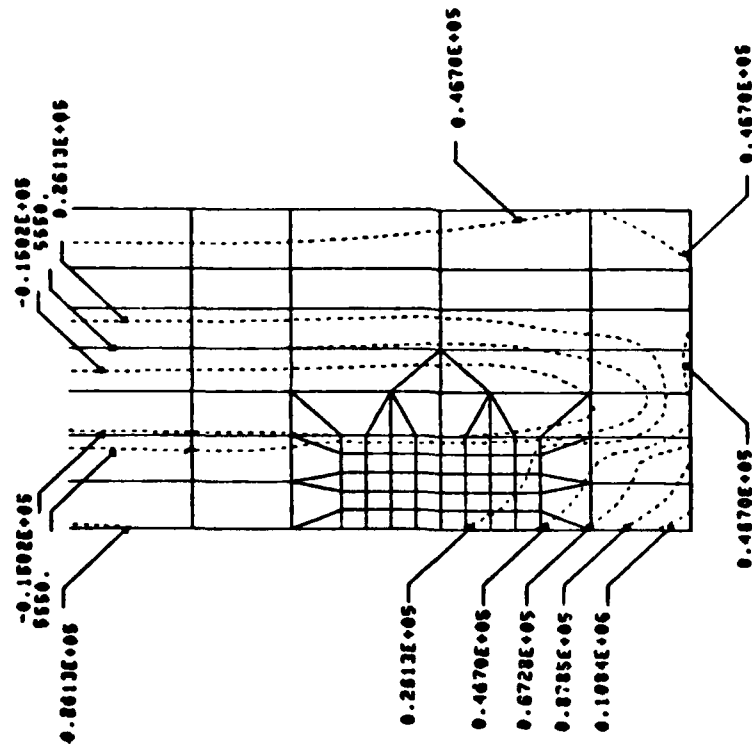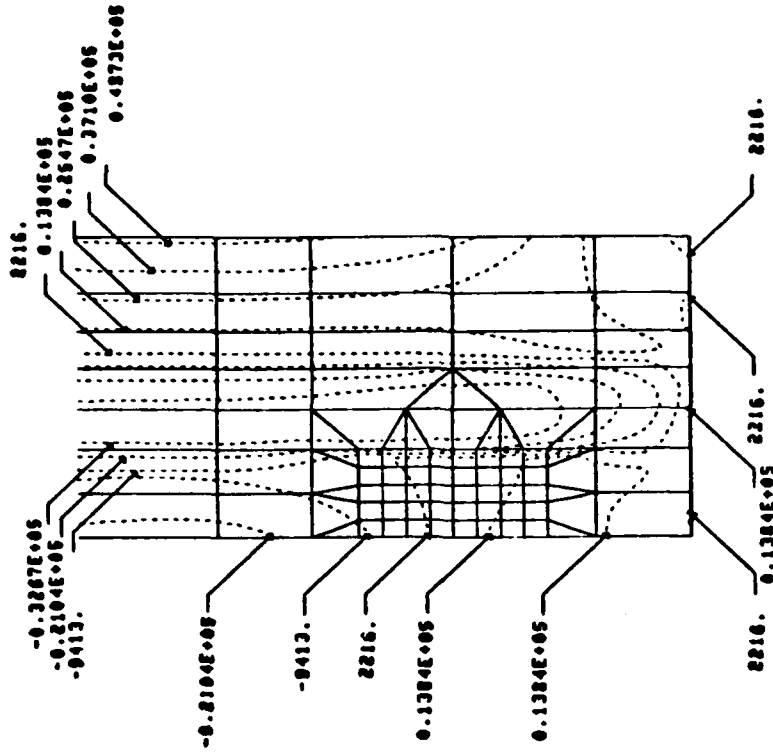

FIGURE 3 – Contour plot of hoop stress due to shrink fit and firing with an α-SiC liner

57

FIGURE 6 – Contour plot of axial stress due to shrink fit and firing with a Si_3N_4 liner

FIGURE 5 – Contour plot of hoop stress due to shrink fit and firing with a Si_3N_4 liner
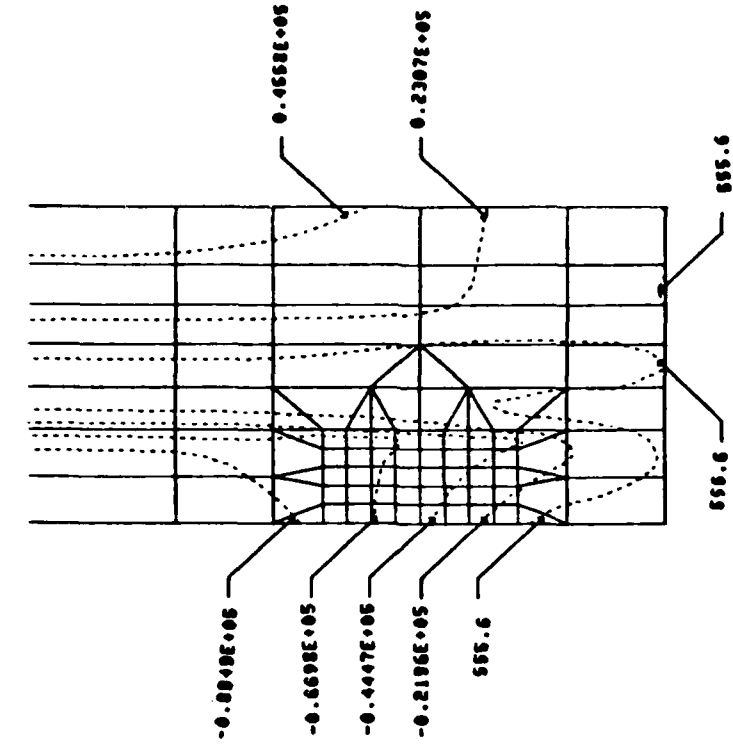
58

FIGURE 8 - Contour plot of axial stress due to shrink fit and firing with a PSZ/TS liner
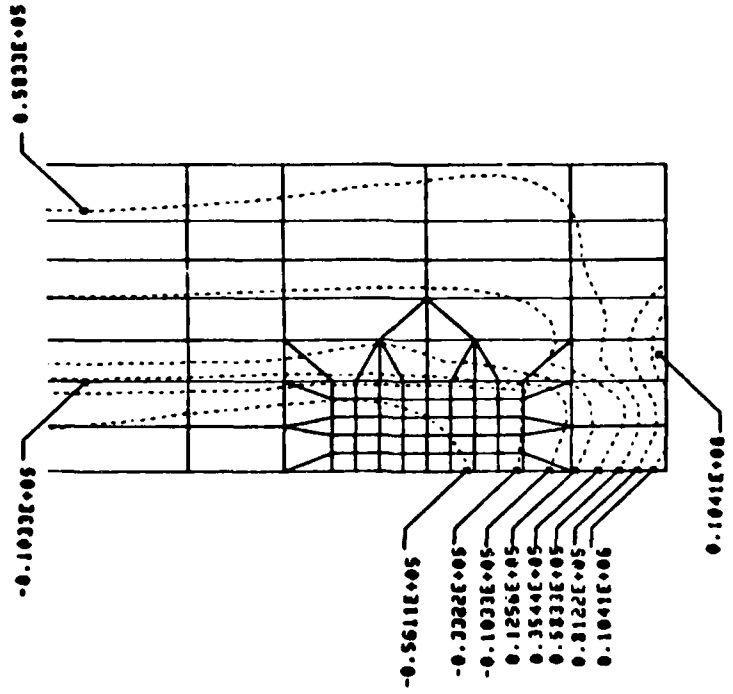

FIGURE 7 - Contour plot of hoop stress due to shrink fit and firing with a PSZ/TS liner

59

AUTHOR INDEX

Artley, M.	Air Force Wright Aeronautical Laboratories	WPAFB, OH
Barsoum, R.	Army Materials Technology Laboratory	Watertown, MA
Bunning, E.	SACO Defense Incorporated	Saco, ME
Burton, L. W.	Army Ballistics Research Laboratory	Aberdeen, MD
Das Gupta, A.	Army Ballistics Research Laboratory	Aberdeen, MD
Freese, C. E.	Army Materials Technology Laboratory	Watertown, MA
Hilton, P.	Arthur D. Little Incorporated	Cambridge, MA
Holmquist, T. J.	Honeywell Incorporated Defense Systems Division	Edina, MN
Johnson, A. R.	Army Materials Technology Laboratory	Watertown, MA
Johnson, G. R.	Honeywell Incorporated Defense Systems Division	Edina, MN
Kaste, R. P.	Army Ballistics Research Laboratory	Aberdeen, MD
Keefe, R. E.	Kaman Sciences Corporation	Colorado Springs, CO
Mayville, R.	Arthur D. Little Incorporated	Cambridge, MA
Murray, R. B.	Army Ballistics Research Laboratory	Aberdeen, MD
Patton, E. M.	Army Ballistics Research Laboratory	Aberdeen, MD
Perrone, P. J.	Army Materials Technology Laboratory	Watertown, MA
Quigley, C. J.	Army Materials Technology Laboratory	Watertown, MA
Reese, E.	Sandia National Laboratories	Albuquerque, NM
Samarase, E.	Columbia University	New York, NY
Severyns, K.	Air Force Wright Aeronautical Laboratories	WPAFB, OH
Shinozuka, M.	Columbia University	New York, NY
Spiridigliozzi, L.	Army Materials Technology Laboratory	Watertown, MA
Sulcoski, M. F.	University of Virginia	Charlottesville, VA
Tessler, A.	Army Materials Technology Laboratory	Watertown, MA
Tong, P.	Transportation Systems Center	Cambridge, MA
Tracey, D. M.	Army Materials Technology Laboratory	Watertown, MA
Warren, T.	Arthur D. Little Incorporated	Cambridge, MA
Wong, P.	Army Materials Technology Laboratory	Watertown, MA